Development/Plasticity/Repair

Pool-Specific Regulation of Motor Neuron Survival by Neurotrophic Support

Fabienne Lamballe, Matthieu Genestine, Nathalie Caruso, Vilma Arce, Sylvie Richelme, Françoise Helmbacher,* and Flavio Maina*

Developmental Biology Institute of Marseille-Luminy (IBDML), UMR 6216, CNRS–Inserm–Université de la Méditerranée, Campus de Luminy-Case 907, 13288 Marseille Cedex 09, France

The precise control of motor neuron (MN) death and survival following initial innervation of skeletal muscle targets is a key step in sculpting a functional motor system, but how this is regulated at the level of individual motor pools remains unclear. Hepatocyte growth factor (HGF) and its receptor Met play key developmental roles in both muscle and MNs. We generated mice (termed "*Nes-Met*") in which *met* is inactivated from midembryonic stages onward in the CNS only. Adult animals showed motor behavioral defects suggestive of impaired innervation of pectoral muscles. Correspondingly, in neonatal spinal cords of *Nes-Met* mutants, we observed death of a discrete population of *pea3*-expressing MNs at brachial levels. Axonal tracing using *pea3* reporter mice revealed a novel target muscle of *pea3*-expressing MNs: the pectoralis minor muscle. In *Nes-Met* mice, the pectoralis minor pool initially innervated its target muscle, but required HGF/Met for survival, hence for proper maintenance of muscle innervation. In contrast, HGF/Met was dispensable for the survival of neighboring Met-expressing MN pools, despite its earlier functions for their specification and axon growth. Our results demonstrate the exquisite degree to which outcomes of signaling by receptor tyrosine kinases are regulated on a cell-by-cell basis. They also provide a model for one way in which the multiplicity of neurotrophic factors may allow for regulation of MN numbers in a pool-specific manner.

Introduction

Despite their shared overall function, neuronal classes comprise distinct subtypes, each of which reflecting functional characteristics, including anatomical position, molecular identity, and specific connectivity. How each subpopulation is generated during development at the correct time and place, and how appropriate numbers are maintained, are therefore critical issues for understanding neural development.

As an example of functional diversity, spinal motor neurons (MNs) are organized into discrete longitudinal columns that segregate spatially into motor pools, the groups of MNs that innervate individual skeletal muscles (Landmesser, 1978; Jessell, 2000). Motor pools differ in MN numbers they contain, which reflect the volume of the target muscle and the number of muscle fibers innervated by each MN. Differences in final pool size are influenced by the initial MN number generated and by the fraction lost through subsequent developmental cell death. This adjustment of MN numbers within pools to the size of target muscles—numerical matching—involves the loss of a fraction of the MNs initially produced, during a specific developmental phase called naturally occurring cell death (NOCD) period, which peaks around E13.5 in mouse. This peak of cell death coincides with the moment when MNs become dependent on muscle-derived factors for survival, as deduced from the timing of MN elimination in mice with impaired muscle development (Fig. 1) (Kablar and Rudnicki, 1999). While some mechanistic origins of differences in initial MN numbers are known (Dasen and Jessell, 2009; Kanning et al., 2010), evidence for pool-specific regulation of MN survival is still lacking, despite the plethora of factors exerting trophic support on cultured MN subsets (Henderson, 1996; Oppenheim, 1996).

In this study, we focused on HGF and its receptor Met, which play complex developmental roles in the neuromuscular system (Maina and Klein, 1999). HGF elicits survival response on MN subsets *in vitro*, and Met is selectively expressed in distinct motor pools (Fig. 1) (Ebens et al., 1996; Yamamoto et al., 1997; Helmbacher et al., 2003). Moreover, anti-HGF blocking antibodies abolish a muscle-derived neurotrophic activity. Several functions of HGF/Met additionally impact on MN biology: at early developmental stages, HGF is required for myoblast migration

Received May 3, 2011; accepted May 27, 2011.

Author contributions: F.L., F.H., and F.M. designed research; F.L., M.G., N.C., V.A., S.R., F.H., and F.M. performed research; F.L., F.H., and F.M. analyzed data F.L., F.H., and F.M. wrote the paper.

This work was supported by funds from the Fondation pour la Recherche Médicale (FRM), Association Française contre les Myopathies (AFM), Fondation de France, Institut National du Cancer, Association pour la Recherche contre le Cancer, and Fondation Bettencourt-Schueller to F.M., and AFM, FRM (Equipe FRM), and Agence Nationale de la Recherche (ANR Neuro 2007) to F.H. M.G. was supported by a University Franco-Italy fellowship. We are particularly grateful to Chris Henderson (Motor Neuron Center, Columbia University) for his remarkable contribution and support; Aziz Moqrich and all members of our laboratories for helpful discussions and comments; Virginia Girod-David and Leo Jullien for excellent help with mouse husbandry at the Developmental Biology Institute of Marseille-Luminy (IBDML); staff at the IBDML and Mediterranean Institute of Neurobiology animal house, transgenic facilities, and imaging platform for technical support; S. Thorgeirsson (NCI) for providing the met^{fl} mouse line; and Laura Loschek for graciously providing data from Nestin-cre;Ret-Flox mice. We thank Drs. Yingbin Ouyang and Richard Coffee (Xenogen Biosciences) for constructing the Etv4-GFP BAC transgene and for microinjections to produce the transgenic animals; and the Institut Clinique de la Souris for mutant ES cell generation and blastocyst injection to produce $Met^{stop\text{-}LacZ/+}$ reporter mice.

The authors declare no competing financial interests.

*F.H. and F.M. contributed equally to this work.

Correspondence should be addressed to either Flavio Maina or Françoise Helmbacher, Developmental Biology Institute of Marseille-Luminy, Campus de Luminy-Case 907, 13288 Marseille Cedex 09, France, E-mail: Flavio.Maina@ibdml.univmed.fr or Francoise.HELMBACHER@ibdml.univmed.fr.

DOI:10.1523/JNEUROSCI.2198-11.2011

 0270-6474/11/3111144-15$15.00/0

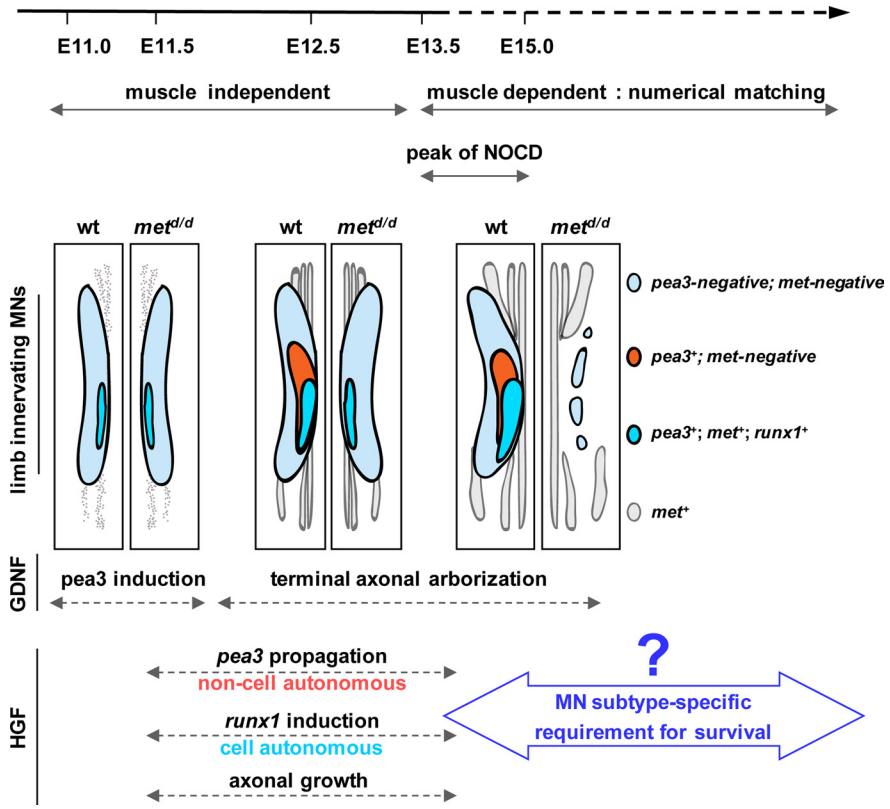

Figure 1. Time course of developmental events regulating biology of MNs. Schematic representation of (1) the relationship between regulation of MN survival and the period of NOCD, (2) the motor pools expressing Met, and (3) the developmental events regulated by the HGF/Met system in brachial MNs as established from the analysis of $met^{d/d}$ mutants. The scheme positions the time when MNs acquire their dependency on muscle-derived trophic factors, opening a phase of numerical matching between the size of motor pools and that of their target muscles. This timing is deduced from the excessive MN death occurring in $met^{d/d}$ mutants where limb muscle development is impaired. The scheme also summarizes the different developmental events regulated by HGF/Met functions in MNs (based on Helmbacher et al., 2003). Before NOCD, HGF/Met is required for axonal growth, for induction of Runx1 expression in Met-positive neurons (cell autonomously), and for the propagation of Pea3 expression from Met-positive to Met-negative MNs (non-cell-autonomous function). After NOCD (E15.5), depletion of limb muscles in $met^{d/d}$ mutants causes the massive loss of all limb innervating MNs (whether they express Met or not). This had prevented so far using the HGF/Met system to study subtype-specific MN survival in response to selective trophic support. This question is the aim of the present study (blue arrow).

from somites to limbs (Bladt et al., 1995; Maina et al., 1996). In *hgf* or *met* null mutants, absence of limb muscles results in trophic support depletion, hence causing death of all limb-innervating MNs (Fig. 1) (Helmbacher et al., 2003). Besides, HGF/Met control early MN specification by regulating expression of the *pea3* transcription factor, and subtype-specific motor axon growth (Ebens et al., 1996; Maina et al., 1997, 2001; Caton et al., 2000; Helmbacher et al., 2003).

The subtype-specific action of HGF/Met led us to use this system for exploring *in vivo* whether MN subgroups depend on distinct trophic support, by combining two novel transgenic lines with four previously described mutants. We demonstrate that an individual motor pool requires a specific neurotrophic factor for its survival, and show that MNs switch their dependency for a given trophic factor in time and for defined biological functions in a pool-specific manner.

Materials and Methods

Animals and genotype analysis

All experimental procedures were performed according to the European Union and institutional guidelines for the care and use of laboratory animals, and were approved by an official committee. Mice were housed under a 12 h light/dark cycle, with dry food and water available *ad libitum*. For behavioral studies, we used adult (2–3 months old) male transgenic mice. The *Nes-Met* mutants were obtained through a genetic setting combining a conditional *met* allele [met^{fl} (Huh et al., 2004)], a signaling-deficient *met* allele [met^{d} (Maina et al., 1996, 1998)], and a strain in which Cre recombinase expression is driven by the nervous system-specific enhancer of *nestin* (Tronche et al., 1999). To generate the $Met^{LacZ/+}$ mice, a *loxP*-flanked-*neo*-stop cassette has been inserted into exon 12 of the *met* locus, resulting in a loss of function of the *met* gene. An *IRES-nls-LacZ-pA* targeting cassette was integrated into exon 12, so that expression of the β-gal reporter is conditioned by the excision of a *neo*-stop cassette. The targeting vector was electroporated into P1 ES cell lines (Institut Clinique de la Souris). Cell recombinants were screened with an external probe on SacI-digested genomic DNA. Oligonucleotides used for PCR screening were as follows: 5′-CAAGCCGAATCACCAAACACTAAGG-3′ (oligo 1), 5′-CCAAGCTGATCCTCTAGAGTCGAC-3′ (oligo 2), 5′-CATCAGAAGCTGACTCTAGAGG-3′ (oligo 3), and 5′-GAATAGT CATGACGTCATCAGC-3′ (oligo 4).

The Etv4-GFP BAC transgenic line was constructed in the research facility of Xenogen Biosciences. Construction began by isolation of the BAC RP24-79P16 (obtained from BACPAC Resources Center, CHORI), containing the murine *Etv4* locus and its putative regulatory environment. The BAC-recombineering technology was used to originate a transgenic BAC, in which an EGFP cassette was inserted into the *Etv4* locus of the BAC (Gong et al., 2002). The EGFP shuttle cassette was designed to generate an in-frame fusion of the EGFP with exon 9 of *Etv4*, leading to a *Etv4-GFP* fusion transcript, and to replace exons 10–13 of *Etv4* in the BAC, such that the *Etv4* locus is knocked out [strategy similar to that applied for Etv4 knock-out by (Livet et al., 2002)] and does not lead to exogenous expression of a functional PEA3 protein. Pronuclear injections of the BAC transgene was performed in the B6SJL (hybrid) mouse strain, and 14 transgenic founder mice were obtained. The basis for selecting one transgenic founder from which to expand the *Etv4-EGFP* mouse line included a screening of the progeny of each transgenic founder for EGFP reporter expression at embryonic stages E12.5 or E13.5. The selected line (founder male number 4) shows an EGFP staining pattern that recapitulates *pea3* expression in the spinal cord and in other tissues, and is detectable in direct fluorescence. The official international name to be used is Tg(Etv4-EGFP)4Hel. Transgenic mice are identified by genomic PCR with the following primers: *pea3*-a1 5′-GGAATCTTGGGCCTTGAGAACAGC-3′; *GFP*-rev 5′-CGCTGAAC-TTGTGGCCGTTTACG-3′. Other mouse lines used in this study were *Del-Ret* and *Nes-Ret* (Kramer et al., 2006). Mice carrying the $runx1^{LacZ}$ allele were obtained from Marella de Bruijn (John Radcliffe Hospital, Oxford, UK), with permission of Nancy A. Speck (University of Pennsylvania, Philadelphia, PA) and genotyped as described by North et al. (1999). Mice carrying the *pea3* null allele ($Etv4^{tm1Arbr}$ allele) were obtained from Silvia Arber, and genotyped as previously described (Livet et al., 2002).

Embryonic MN cultures

E12.5 mouse embryos were collected in Hibernate medium (Invitrogen) with B-27 supplement (Invitrogen), and kept on ice until dissection, while the genotype was determined by PCR. Ventral spinal cords from an equal number of wild-type and $met^{d/d}$ mutant embryos were dissected.

MNs were isolated either from brachial + lumbar or from cervical + thoracic + sacral segments, by a previously described method (Arce et al., 1999), involving a combination of BSA cushion centrifugations and a metrizamide density gradient centrifugation. At the end of the procedure, the cell suspension is highly enriched in MNs. Cells were then plated in polyornithine/laminin-coated four-well tissue culture dishes for survival experiments (1500 neurons per well) in Neurobasal medium. Recombinant neurotrophic factors were added 2 h after seeding. MNs were kept for 3 d either in Neurobasal medium or in the presence of GDNF or HGF (both obtained from R&D). MN survival was quantified by counting large, bright unipolar neurons with long axonal processes on the whole area of each well.

In situ *hybridization and quantification of MN numbers*

In situ hybridization on whole-mount embryos were performed as previously described (Maina et al., 1996, 2001). Spinal cords were dissected at the appropriate stage, with long spinal roots, allowing unambiguous identification of every spinal segment, and fixed overnight in 4% PFA. Fragments of spinal cords including the C5–T2 segments were frozen in PBS, 20% sucrose, and 7.5% gelatin, and cryosectioned (16 μm) transversally. *In situ* hybridization studies on whole-mount spinal cords or cryosections were performed as previously described (Helmbacher et al., 2003). Riboprobes used in this study were for *met* (Yamamoto et al., 1997), *pea3* (from T. Jessell, Columbia University, New York, NY), *sema3E* (from J. Livet, The Vision Institute, Paris, France), *runx1* (clone IRAKp961C01148Q, ImaGenes), and choline acetyltransferase (*ChAt*) (from C. Henderson, Columbia University, Motor Neuron Center, New York, NY). Quantitative analysis was performed by counting the number of *ChAt*-, *pea3*-, or *runx1*-positive MNs on one of every four sections throughout the entire length of the C5–T2 region. Presence or absence of dorsal roots allowed us to determine precisely the anteroposterior coordinates of each section. For each mice group, each side of the spinal cord sections was counted separately.

β-Galactosidase staining

X-gal staining was performed according to standard techniques on whole embryos or dissected spinal cords. For $Met^{LacZ/+}$ or $runx1^{LacZ/+}$ motor neuron counts, dissected spinal cords were fixed 2 h in 4% PFA and C5–T2 spinal segments were then embedded in gelatin/albumin. Fifty-micrometer-thick vibratome serial cross sections were collected and subjected to X-gal staining. LacZ-positive MNs were counted on all sections. For each genotype, left and right sides of the spinal cord sections were counted separately. As described for the *in situ* hybridization, the anteroposterior coordinates of each section was determined thanks to the presence of the spinal segments.

Immunohistochemistry

Immunostaining of embryos were performed as previously described (Maina et al., 2001). Whole-mount immunohistochemistry on muscles was done as described previously (Livet et al., 2002). Antibodies and reagents used were as follows: anti-neurofilament (α-NF-M, 1:400), anti-Tau (1:50), anti-GFP (1:500), peroxidase-conjugated anti-rabbit antibodies (1:200), Alexa 555-conjugated anti-rabbit (1:400), Alexa 488-conjugated anti-chicken (1:500), and Alexa 594-conjugated phalloidin (1:40). For whole-mount immunohistochemistry, pectoralis minor and pectoralis major muscles were dissected, fixed in Dent's solution overnight, and subjected to immunohistochemistry using anti-NF antibodies. Peroxidase activity of the secondary antibody was developed with DAB (Sigma). Each muscle was imaged in two stereotyped positions (clavicular and thoracic regions) at 10× magnification. Two-dimensional scoring of axonal arborization was performed using the NeuronJ plugin (Meijering et al., 2004) to ImageJ software (NIH), by drawing axon branches following the observable pattern, and plotting separately the length and number of branches, with each dot representing data from individual muscle. For analysis of neuromuscular junctions (NMJs), dissected muscles were fixed in 4% PFA (20 min), cryoprotected in 15% sucrose overnight at 4°C, and then frozen in 15% sucrose/7.5% gelatin. Forty-micrometer-thick longitudinal cryostat sections were collected on glass slides. They were first stained for 1 h in Alexa 488-conjugated α-bungarotoxin (BTX, 1:1000), then washed in PBS/0.1% Triton, permeabilized in methanol for 5 min at −20°C, washed, and subjected to standard immunohistochemistry with anti-NF or anti-Tau antibodies (P2 or adult, respectively). NMJs were observed under a Zeiss Axioplan microscope equipped with Apotome, and classified as follows: "completely innervated": the end-plate totally overlapped with the axon terminal; "denervated": the end-plate was not associ-

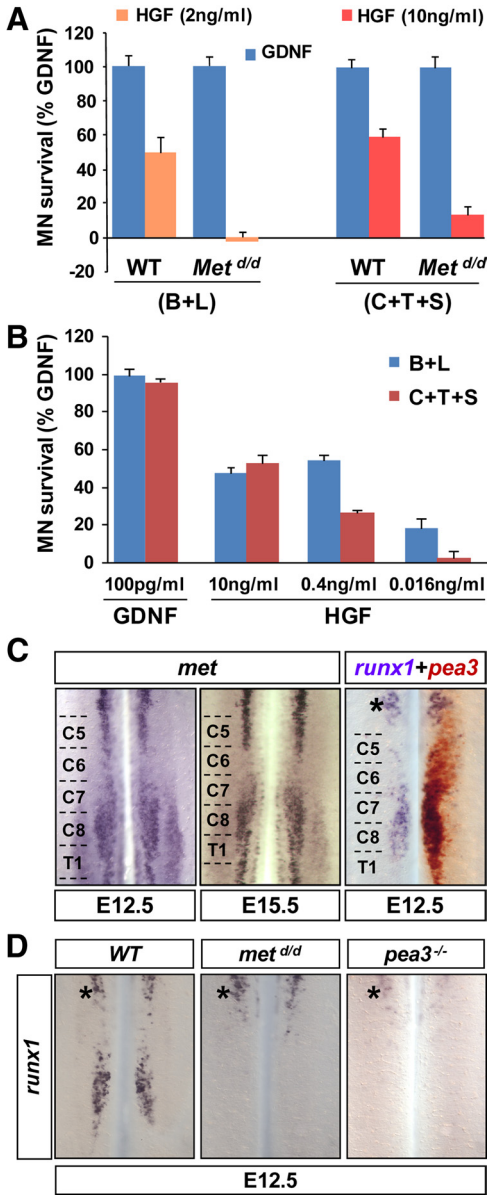

Figure 2. Requirement of a subpopulation of MNs to HGF. ***A***, Survival of MNs derived from E12.5 spinal cords of wild-type (WT) and $met^{d/d}$ embryos in presence of GDNF (100 pg/ml) or HGF. Survival values are expressed as percentage of MN response to GDNF (defined as 100%). The HGF trophic support has been tested at 2 ng/ml on MNs derived from brachial and lumbar (B+L) regions, or at 10 ng/ml on MNs derived from the cervical+thoracic+sacral (C+T+S) spinal segments. No significant survival response by HGF was observed on $met^{d/d}$ MNs. ***B***, Survival of MNs isolated from either brachial+lumbar (B+L), or from cervical+thoracic+sacral (C+T+S) spinal segments of E12.5 embryos in presence of GDNF (100 pg/ml) or various doses of HGF. Results are expressed as percentage of response to GDNF (defined as 100%). HGF exerts its trophic support at lower concentration in (B+L) MNs as compared to (C+T+S) MNs. ***C***, Met expression domain in E12.5 and E15.5 spinal cords revealed by *in situ* hybridization on whole-mount wild-type spinal cords using the *met* riboprobe. Positions of the C5–T1 spinal segments are indicated. Right, Double *in situ* hybridization performed at E12.5 showing the expression domain of *runx1* (purple) and *pea3* (red). The same spinal cord side is shown twice, mirror imaged, before and after developing the *pea3* (red) staining. ***D***, *In situ* hybridization performed at E12.5 showing loss of *runx1* expression in the *pea3* region in $met^{d/d}$ and $pea3^{-/-}$ spinal cords. The asterisk indicates that *runx1* expression is maintained in both mutants outside the *pea3* domain.

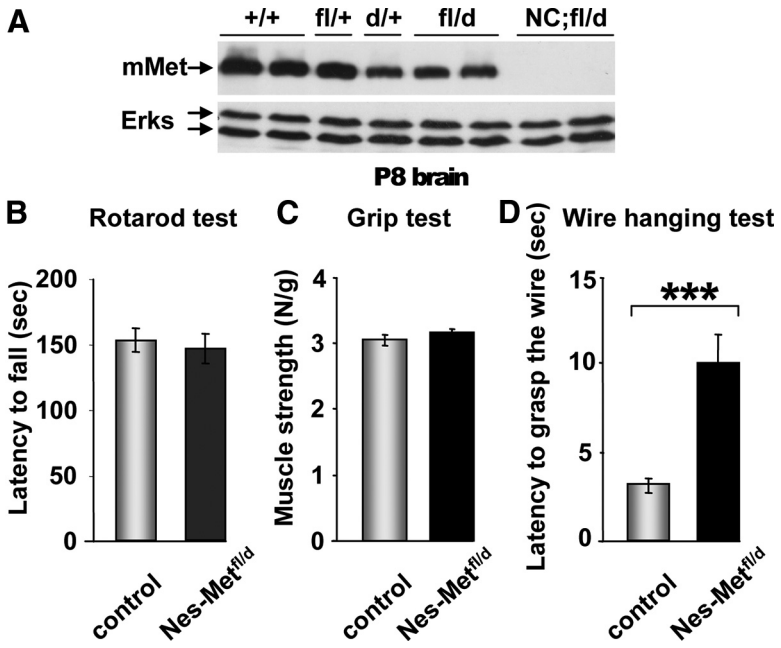

Figure 3. Specific motor performance defects in adult *Nes-Met*$^{fl/d}$ mutants. ***A***, Western-blot analysis of Met expression levels in whole-brain extracts of control (+/+, fl/+, d/+, fl/d) and mutant (*Nes-Met*$^{fl/d}$, indicated as NC;fl/d) P8 mice. Mouse Met protein (mMet) is totally absent in mutant brains. Reprobing the membrane with antibodies to total ERKs is used as loading control. ***B***, Rotarod studies showing that the latency to fall off from the rod was not significantly different between controls (*Nes-Met*$^{fl/+}$; $n = 18$) and *Nes-Met*$^{fl/d}$ mutants ($n = 17$). ***C***, Grip test studies revealing that no significant differences were observed between controls (*Nes-Met*$^{fl/+}$; $n = 29$) and *Nes-Met*$^{fl/d}$ mutants ($n = 38$). The muscle strength developed by each animal was expressed in newtons and normalized to the body weights of each mouse (in grams). ***D***, Wire hanging behavioral test indicating that the latency to grasp the wire by at least one of their hindpaw was significantly higher in the *Nes-Met*$^{fl/d}$ mutants ($n = 38$) compared to controls (*Nes-Met*$^{fl/+}$; $n = 29$). ***$p < 0.001$. Error bars represent SEM.

ated with an axon. In case of partial overlap, the NMJ was scored as "partially innervated."

To perform imaging of the EGFP fluorescence in Etv4-GFP-derived material, tissues were shortly fixed in 4% PFA. Spinal cords were dissected from E12.5 embryos before 15 min fixation, while muscles were dissected from E12.5 or E17.5 embryos previously fixed for 15 or 30 min, respectively. All tissues were rinsed three times in PBS. Muscles were further incubated in PBS supplemented with Alexa 594-conjugated α-bungarotoxin (1:1000) for 30 min, and rinsed again three times in PBS, before direct imaging of the GFP fluorescence. Double immunofluorescence with anti-NF (red) and chicken-anti-GFP (green) were performed as described above on dissected pectoralis minor muscles. All samples were mounted on slides with Prolong Gold Antifade Kit (Invitrogen). Image acquisition was performed with a Zeiss Axioplan equipped with Apotome.

Antibodies and reagents

Antibodies used were anti-tubulin (Sigma), anti-mouse Met (B-2; sc-8057, Santa-Cruz), anti-neurofilament (rabbit anti-NF AB1987, Millipore, and mouse anti-NF155 kDa clone 2H3 from Developmental Studies Hybridoma Bank), anti-Tau (Ab8763, Abcam), chicken-anti-GFP (Aves Labs), anti-rabbit peroxidase- or Cy3-coupled secondary antibodies (Jackson ImmunoResearch Laboratories), and anti-chicken Alexa 488 and anti-rabbit Alexa 555-coupled secondary antibodies (Invitrogen). Other reagents were Alexa 488- or Alexa 594-conjugated α-bungarotoxin and Alexa 594-coupled phalloidin (Invitrogen).

Western immunoblotting

Protein extracts were prepared from freshly dissected spinal cords at the appropriate stages and Western-blot analyses were performed as previously described (Segarra et al., 2006; Moumen et al., 2007a,b; Furlan et al., 2011).

Behavioral tests

The behavioral tests used in this study aimed at measuring motor abilities of the conditional *Nes-Met* mutant mice. They allowed evaluating motor coordination (rotarod) and muscular strength (grip and wire hanging tests). All animals used for this study were 2–3 months old.

Rotarod test. The rotarod test, using an accelerating rotarod, was performed by placing mice on rotating drums (3 cm diameter) and measuring the time each animal was able to maintain its balance on the rod. The speed of the rotarod accelerated from 4 to 40 rpm over a 5 min period.

Grip test. The grip strength of each animal was measured using an isometric dynamometer connected to a grid (Bioseb). Each mouse was made to grasp the grid with its forepaws, and was slowly pulled back by the tail until release of the grid. The maximal strength developed was recorded and expressed in newtons. Five individual trials were performed for each mouse, and the average value was used for statistical analysis.

Wire hanging test. The apparatus was a wire stretched horizontally 40 cm above a table. Testing consisted of three consecutive trials separated by 30 min interval. On each trial, the forepaws of the animal were placed on the thread. The latency the animal took to catch the wire by one of its hindpaws was recorded (60 s maximum). If the animal fell down, it was credited with 60 s.

Statistical analysis

All data are presented as mean ± SEM. Data were analyzed with Student's t test. p values >0.05 were considered nonsignificant. *$p < 0.05$, **$p < 0.01$, ***$p < 0.001$.

Results

Subtype-specific regulation of spinal MN survival by HGF/Met

Given the plethora of factors with neurotrophic properties, and the combinatorial, pool-specific expression of their receptors, could one given target-derived factor be necessary and sufficient for the survival of a limited subset of MN pools? Although HGF is produced by most muscles (Gu and Kania, 2010), the restricted expression of Met in subsets of MN pools may reflect their specific dependency on HGF/Met signaling for survival. HGF was previously reported to support primary embryonic MN survival *in vitro* (Ebens et al., 1996; Wong et al., 1997; Yamamoto et al., 1997; Novak et al., 2000; Koyama et al., 2003), and *in vivo* in ALS animal models (Genestine et al., 2011). However, the massive elimination of limb-innervating MNs resulting from migratory muscle depletion in Met mutants occurs whether or not MNs express Met. While this defined the onset of the muscle-dependent period (Fig. 1), it precluded so far using the HGF/Met system to obtain *in vivo* evidence of pool specific requirement to a given trophic signal.

To first obtain *in vitro* genetic evidence that Met is required for the survival response to HGF, we used primary mouse MN cultures derived from wild-type or *met*$^{d/d}$ signaling mutant embryos. The response to HGF was assessed for both limb-innervating (brachial + lumbar; B+L) and non-limb-innervating (anterior cervical + thoracic + sacral; C+T+S) segments. At either level,

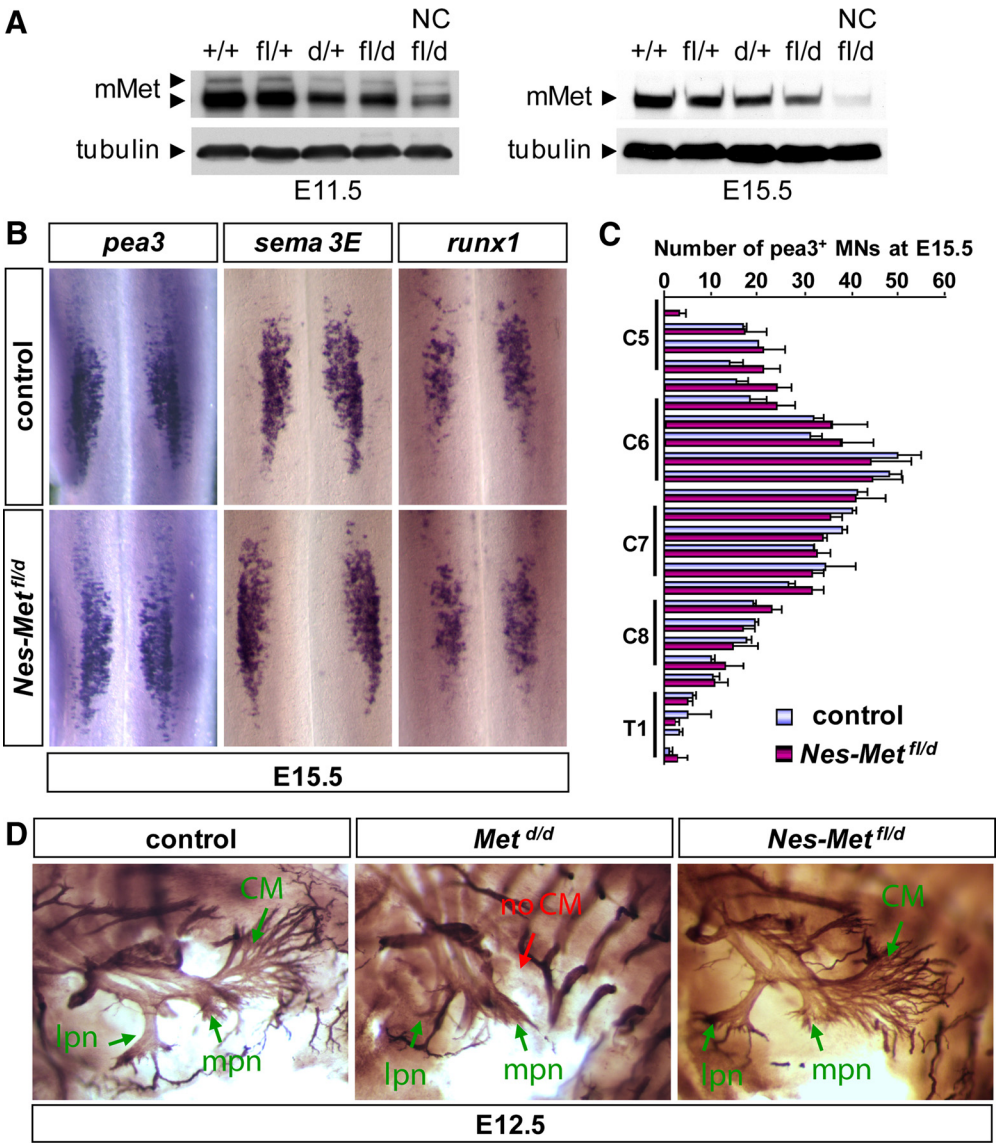

Figure 4. Met-dependent specification and axon guidance are preserved in *Nes-Met*$^{fl/d}$ mutants. ***A***, Western-blot analysis of Met expression levels in whole spinal cord extracts of E11.5 and E15.5 control (+/+, fl/+, d/+, fl/d) and mutant (NC;fl/d) embryos. Mouse Met protein (mMet) is still present at E11.5, while its level is largely reduced at E15.5. ***B***, Whole-mount *in situ* hybridization of E15.5 spinal cords using *pea3*, *sema3E*, and *runx1* riboprobes. At E15.5, no changes in the expression domain of any of these genes are apparent in *Nes-Met*$^{fl/d}$ mutants ($n = 2$) as compared to controls (*Nes-Met*$^{fl/+}$; $n = 2$). ***C***, Quantification of *pea3*-positive MNs at E15.5, showing similar MN numbers in *Nes-Met*$^{fl/d}$ mutants versus controls (*Nes-Met*$^{fl/+}$). Positions of C5–T1 dorsal root ganglia (DRGs) are indicated by vertical black lines. Error bars represent SEM. ***D***, Whole-mount anti-neurofilament staining of E12.5 embryos at the forelimb level (dorsal up, anterior left). Lateral and medial pectoral nerves (lpn and mpn, respectively) are unchanged by *met* deletion, whereas the cutaneous maximus nerve shows a pronounced axonal growth defect in *Met*$^{d/d}$, but not in *Nes-Met*$^{fl/d}$ mutants.

only a fraction of MNs survived in presence of HGF (Fig. 2*A*), likely reflecting the expression of Met by subsets of MNs *in vivo*. In *met*$^{d/d}$ signaling mutants, the effect of HGF on cultured MNs was lost, as expected (Fig. 2*A*). Interestingly, as reported with rat MNs (Yamamoto et al., 1997), the HGF concentrations required for efficient support of non-limb-innervating medial motor column neurons, in which Met is also expressed, are higher than those required for brachial and lumbar lateral motor column neurons (B+L: 0.4 ng/ml; C+T+S: 10 ng/ml) (Fig. 2*B*) (Yamamoto et al., 1997), suggesting a greater dependence of limb-innervating MNs on HGF for their survival. Consistently, no excessive loss of MNs was observed in *met*$^{d/d}$ spinal cords outside lateral motor columns at E15.5 (just after the NOCD period), excluding any major requirement for HGF/Met for their survival, at least at this stage.

We therefore set out to characterize how Met expression among brachial MN subsets might be relevant for survival. As previously shown, in the brachial spinal cord at E12.5, *met* expression is restricted to some motor pools, including those located in the most posterior region of the *pea3* domain (Fig. 2*C*) (Helmbacher et al., 2003). This expression is maintained at E15.5, after the peak of NOCD (Fig. 2*C*) (Yamamoto et al., 1997). In addition to expression in medial/hypaxial motor columns at cervical and thoracic levels, high levels of *met* are detected in MNs corresponding to the posterior (C7–T1) part of the *pea3* domain (Fig. 2*C*) (Helmbacher et al., 2003). Thus, a differential HGF response of MN subgroups combined with the restricted expression of *met* in subsets of lateral motor column pools in the brachial region suggested that MN pool might vary in their requirements for trophic support *in vivo*.

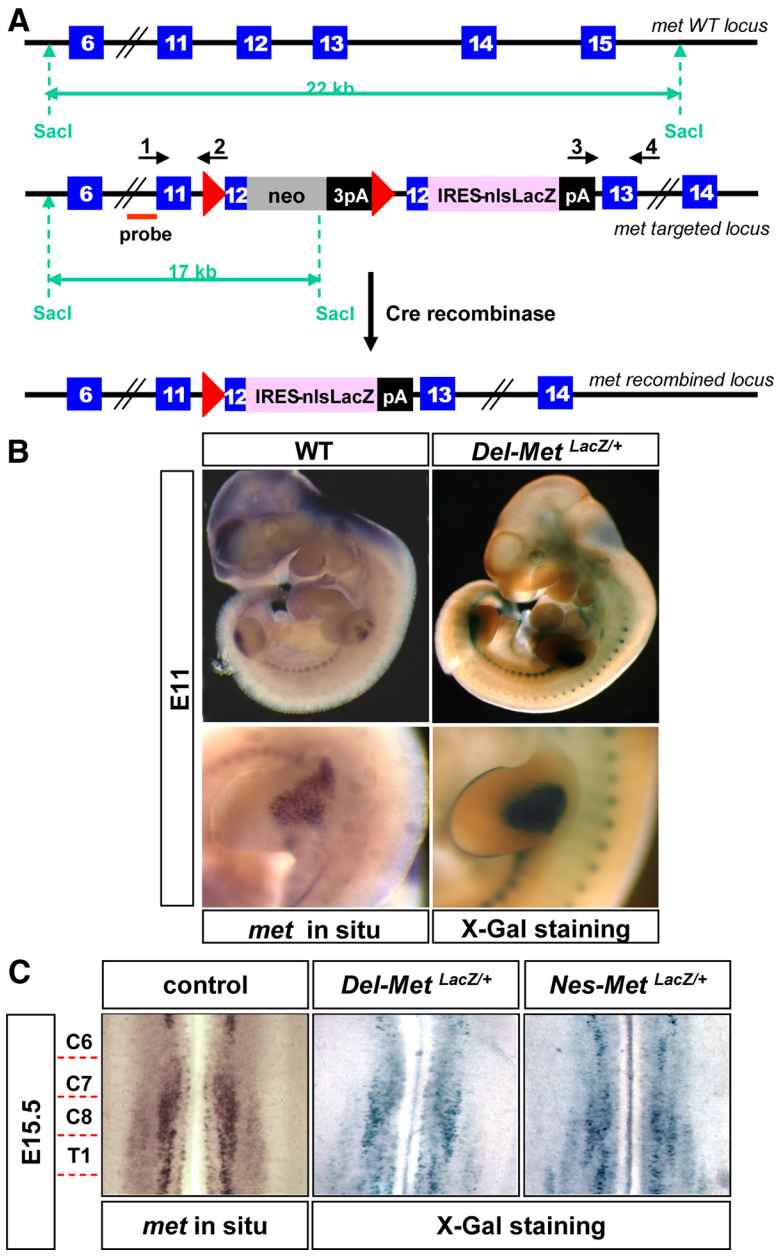

Figure 5. Generation and characterization of conditional $Met^{LacZ/+}$ reporter mice. ***A***, Schematic representation of the targeting strategy used to generate the met^{LacZ} allele. The knock-in insertion of the stop cassette followed by the *lacZ* reporter gene into the *met* locus results in a loss of function of the *met* gene. Expression of the *lacZ* gene is conditioned by the excision of a loxP-flanked-neo-stop cassette, which allows labeling Met-positive cells. Blue boxes indicate exons 6–14 of the *met* locus. Exon 12 encodes the transmembrane domain of the Met protein. *loxP* sites are represented by red arrowheads. The neo cassette consists of the *neomycin* resistance gene followed by three copies of the SV40 polyadenylation signal (3pA). The IRES-nlsLacZ cassette is shown by the pink box (nls: nuclear localization signal). Position of the probe and primers used for selection of targeted embryonic stem (ES) cell clones is indicated. ***B***, The expression of the LacZ reporter knocked into the *met* locus is conditioned by the excision of a stop cassette. When the Cre recombinase is ubiquitously expressed ($Del\text{-}Met^{LacZ/+}$), Met expression pattern revealed by β-galactosidase activity fully recapitulates that evidenced by *in situ* hybridization using the *met* riboprobe in whole E11 embryo. The lower panels show Met-positive migrating myoblasts in the forelimb of wild-type and $Del\text{-}Met^{LacZ/+}$ mutants by *met in situ* hybridization and by the β-galactosidase activity, respectively. ***C***, Analysis of the β-galactosidase activity in spinal cords from E15.5 $Del\text{-}Met^{LacZ/+}$ and $Nes\text{-}Met^{LacZ/+}$ mutants. The expression of the *lacZ* reporter in $Del\text{-}Met^{LacZ/+}$ mutants recapitulates the expression pattern of the *met* transcript evidenced by *in situ* hybridization. Positions of the C6–T1 spinal segments are indicated.

Specific motor performance defects in adult conditional *Nes-Met* mutants

To selectively inactivate Met signaling in the nervous system and bypass not only embryonic lethality, but also the muscle migration defect and consequent trophic depletion, we used combinations of three alleles: (1) a conditional *met* allele [met^{fl} (Huh et al., 2004)], (2) a functionally null *met* allele [met^{d} (Maina et al., 1996)], and (3) a strain in which Cre recombinase expression is driven by the nervous system-specific enhancer of *nestin* (Tronche et al., 1999). The resulting conditional knockouts had the genotype $nestin\text{-}cre;met^{fl/d}$ and will be referred to here as $Nes\text{-}Met^{fl/d}$. Western blot analysis showed that $Nes\text{-}Met^{fl/d}$ mutants exhibited complete excision in postnatal brains (Fig. 3*A*). Conditional $Nes\text{-}Met^{fl/d}$ mutants have a normal lifespan and weight curve (not shown), indicating that early functions of Met in placenta or muscle development have been preserved.

Despite their normal lifespan, we asked whether neuronal deletion of Met functions causes a physiological deficit in adult $Nes\text{-}Met^{fl/d}$ mutants by performing behavioral tests focused on specific motor performance. The rotarod behavioral test, which monitors a variety of proprioceptive, vestibular, and fine-tuned motor abilities, excluded any major coordination defects in the $Nes\text{-}Met^{fl/d}$ mutants (Fig. 3*B*). Given the known role of Met signaling in regulating development of brachial motor pools, we next focused on tests that would allow us to measure the functional performance and strength of different groups of upper muscles. The grip test, which relies upon muscles of the forepaws and forearms, did not show any significant difference between adult $Nes\text{-}Met^{fl/d}$ mice and controls (Fig. 3*C*). In contrast, the wire hanging test, which involves recording the time the animal takes to lift up its trunk so that it can catch the wire by one of its hindpaws, revealed a clear functional defect in the $Nes\text{-}Met^{fl/d}$ mutants (Fig. 3*D*). Notably, a number of $Nes\text{-}Met^{fl/d}$ mice were capable of holding the wire and eventually grasping it with their hindpaws, whereas others were not able to hang on the wire and were falling down, indicating a variability of the severity of the phenotype. The specific performance defects uncovered by the wire hanging test, but not the grip test, suggested defective innervation of some, but not all, forearm and/or pectoral muscle(s), indicating that only a subset of MNs might be affected.

MN specification and axon guidance are preserved in conditional *Nes-Met* mutants

Deciphering the specific dependence of brachial MN subgroups on HGF for survival required that a genetic system also preserves three early neuronal functions of Met. First, Met is required for axonal growth to the Pea3 target muscles cutaneous maximus and latissimus dorsi (Maina et al., 1997, 2001). Second, Met is required non-cell autonomously for ex-

pansion of Pea3 expression, after its initial induction by GDNF (Fig. 1) (Helmbacher et al., 2003). Third, we found that Met (as well as Pea3) is also required for expression of the transcription factor Runx1 (Dasen et al., 2005; Stifani et al., 2008) in the caudal part of the Pea3 domain (C7–C8 levels), where Met is coexpressed (Fig. 2*C*,*D*) (Stifani et al., 2008). Indeed, *runx1* expression was lost at E12.5 in both *pea3*$^{-/-}$ and in the *met* signaling-deficient (*met*$^{d/d}$) mutants (Fig. 2*D*), while it was preserved in both mutants in other, more anterior, cervical motor pools. Runx1 expression distinguishes two subgroups of neurons coexpressing *met* and *pea3*: one *runx1*-positive at C7–C8 levels, and a second population *runx1*-negative, extending more caudally to T1 (Fig. 2*C*). We reasoned that the *Nes-Met*$^{fl/d}$ mutants could be an appropriate genetic setting to preserve these early Met neuronal functions, as we observed a limited efficiency of the *nestin-cre* transgenic line on Ret deletion in the *pea3*-positive MN population by E12.5 (data not shown and Kramer et al., 2006).

We therefore determined when Met protein expression was extinguished in *Nes-Met*$^{fl/d}$ spinal cords by Western blot analysis and found only slight reduction at E11.5 and E13.5 (Fig. 4*A* and data not shown). By contrast, at E15.5, there was a stronger reduction in levels of Met protein in *Nes-Met*$^{fl/d}$ mutant spinal cords than in those of controls (Fig. 4*A*). Thus, this time course of Met protein depletion might allow preserving its early neural functions and investigating its contribution to MN survival after the peak of NOCD. To confirm this, we first examined expansion of the *pea3* expression domain in *Nes-Met*$^{fl/d}$ mutants, which occurs between E10.5 and E12.5 (Helmbacher et al., 2003). Whole-mount *in situ* hybridization showed normal expression of *pea3* and of its target genes *sema3E* and *runx1* (Fig. 4*B* and data not shown). Moreover, there were indistinguishable numbers of *pea3*-positive MNs in E15.5 *Nes-Met*$^{fl/d}$ mutants and controls (Fig. 4*C*). Second, the characteristic branching pattern of motor axons in the cutaneous maximus, a muscle target of the *pea3*-expressing MNs, was also preserved at E12.5, a stage at which it was totally absent in *met*$^{d/d}$ embryos (Fig. 4*D*). Overall, therefore, our conditional genetic model preserves both the non-neural and early neural functions of Met in the *pea3* domain, namely expansion of *pea3* pools, correct innervation of the *pea3* target cutaneous maximus muscle, and induction of *runx1* expression. Thus, the *Nes-Met*$^{fl/d}$ mice provide a unique tool for genetically exploring the role of Met in MNs after the NOCD period.

One caveat for interpretation of these data was that although we had shown that Met expression was maintained sufficiently at early stages, the degree of Met inactivation at later stages had not been followed on a cell-by-cell basis. To analyze *met* excision in the conditional null mutants, we needed a system to genetically label neurons in which Met is deleted, termed here as recombined-*met* neurons. We therefore generated mice in which a loxP-stop-loxP-lacZ cassette was introduced into the *met* locus (referred to as *Met*$^{stop\text{-}LacZ/+}$). This created not only a loss-of-function allele of *met*, but also a conditional reporter of expression from the *met* locus (Fig. 5*A* and data not shown), since *LacZ* reporter expression is only activated following cre-mediated excision of the floxed stop cassette. We first validated the *Met*$^{stop\text{-}LacZ/+}$ reporter strain by crossing these mice with *deleter-cre* transgenics. We found that, in this context of ubiquitous Cre activity (mice are referred to as *Del-Met*$^{LacZ/+}$), β-galactosidase staining recapitulated the expression pattern of *met* mRNA (Fig. 5*B*). In the spinal cord, β-galactosidase staining at brachial, thoracic, lumbar, and sacral spinal cord levels faithfully reproduced the endogenous mRNA expression pattern in MN columns (Fig. 5*C* and data not shown). The extent of Met deletion driven by the *nestin-cre* allele was

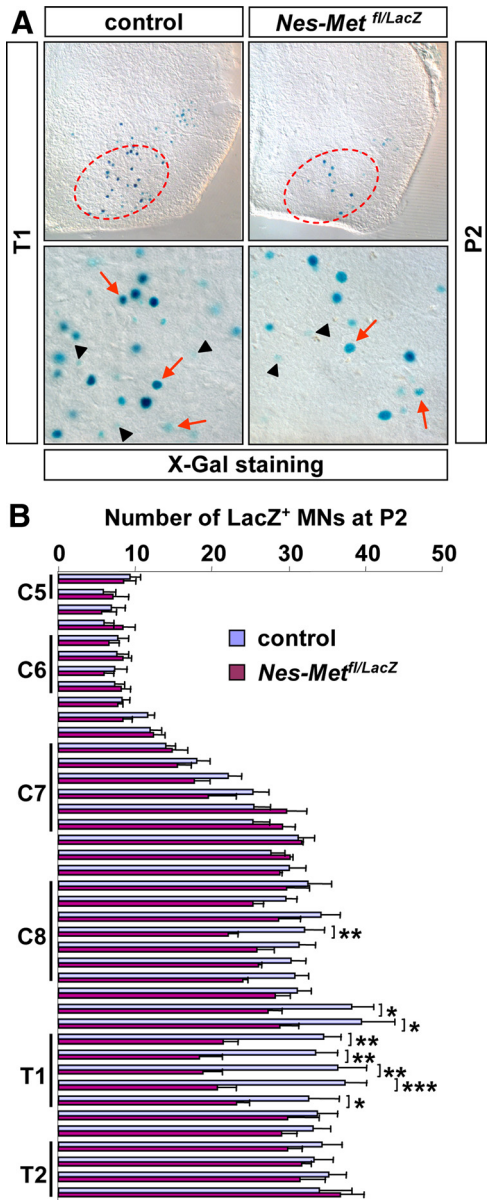

Figure 6. Specific loss of Met-positive motor neurons in the C8–T1 region of *Nes-Met*$^{fl/LacZ}$ mutants. ***A***, Representative images of the ventral horn of the spinal cord showing a reduction of Met-positive cells, identified by the β-galactosidase activity, in the C8–T1 region of the P2 *Nes-Met*$^{fl/LacZ}$ mutants as compared to controls (*Nes-Met*$^{LacZ/+}$). The red dotted line indicates the area where MNs are lost in the *Nes-Met*$^{fl/LacZ}$ mutants. Bottom, High magnification of the pictures showing that at P2 Met is expressed in MNs (red arrows) and at low levels in some glial cells (black arrowheads). ***B***, Quantitative analysis revealing a reduction up to 50% of Met-positive MN numbers in P2 *Nes-Met*$^{fl/LacZ}$ mutants compared to controls (*Nes-Met*$^{LacZ/+}$) within the C8–T1 region. Positions of C5–T2 DRGs are indicated by vertical black lines. Student's *t* test: $*p < 0.05$, $**p < 0.01$, $***p < 0.001$. Error bars represent SEM.

followed by generating *nestin-cre;met*$^{LacZ/+}$ animals (referred to as *Nes-Met*$^{LacZ/+}$). At E15.5, *Nes-Met*$^{LacZ/+}$ embryos displayed a pattern of β-galactosidase activity similar to that seen in *Del-Met*$^{LacZ/+}$ spinal cords and to the pattern of endogenous *met* mRNA expression (Fig. 5*C*). Quantification of *LacZ*-expressing cell numbers on E15.5 *Nes-Met*$^{LacZ/+}$ brachial spinal cord sections revealed that *nestin-cre*-mediated excision occurred in ~80% of MNs as compared to the germline *deleter* strain (C5–C7: 77%; C8–T1: 81.2%; data not shown). These experiments therefore defined conditions for efficient *met* excision in the *pea3* domain at stages after specification, axonal growth, and NOCD

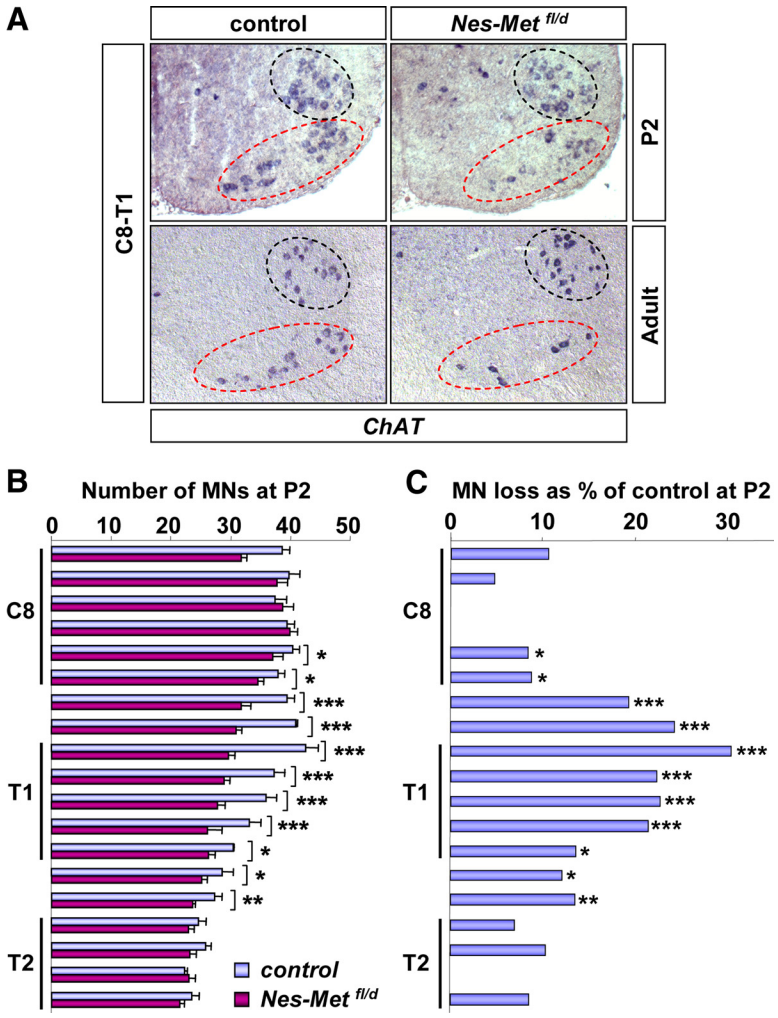

Figure 7. Conditional deletion of the *met* gene results in loss of a specific subpopulation of spinal motor neurons. *In situ* hybridization using a *ChAt* riboprobe was performed on serial cross sections along the anteroposterior axis of the spinal cord brachial region of newborn (P2) or adult *Nes-Met*$^{fl/d}$ mutants and controls (*Nes-Met*$^{fl/+}$) ($n = 6$ for each group of animals). ***A***, High magnification of the ventral horn of the spinal cord shows that at the C8–T1 region, MNs are organized in two groups (dashed lines). The cluster located in the more ventral position exhibits less MNs in the *Nes-Met*$^{fl/d}$ mutant than in controls (red line), whereas the pool of MNs in the more dorsal cluster appears normal (black line). ***B***, Analysis of the brachial region at P2 shows that MN numbers are decreased specifically in the C8–T1 region of the *Nes-Met*$^{fl/d}$ mutants as compared to controls. Positions of the C8, T1, and T2 DRGs are indicated by vertical black lines. ***C***, The reduction of MN numbers shown in ***B*** are expressed as the percentage of MN lost in the *Nes-Met*$^{fl/d}$ mutants versus controls. Student's *t* test: $*p < 0.05$, $**p < 0.01$, $***p < 0.001$. Error bars represent SEM.

peak have occurred, allowing us to investigate for the first time the role of HGF/Met in later stages of MN development.

Fate of MNs following late inactivation of Met

Combining the *met*^{LacZ} null allele with both the conditional *met*^{fl} allele and *nestin-cre* (*Nes-Met*$^{fl/LacZ}$) inactivates *met* and allows the resulting recombined-*met* neurons within the *met*-expression domain to be visualized following X-Gal staining. Analysis of P2 brachial spinal cords revealed that a large proportion of recombined-*met* neurons could be detected in *Nes-Met*$^{fl/LacZ}$ spinal cords (Fig. 6*A*). However, a detailed analysis of their anteroposterior distribution revealed a localized area, restricted to C8–T1 levels, characterized by a ~50% reduction in the number of recombined-*met* neurons in *Nes-Met*$^{fl/LacZ}$ mutants compared to *Nes-Met*$^{LacZ/+}$ controls (Fig. 6*A*,*B*)—therefore likely excluding the most rostral *met*-expressing MNs at C7 level. Moreover, the missing cells appeared to correspond to a group of MNs in a characteristic medioventral position, suggesting that they might correspond to one or more motor pools (Fig. 6*A* and data not shown). In contrast, we found no significant reduction in the number of β-galactosidase-positive neurons at more anterior cervical levels or in any thoracic segments (Fig. 6*B* and data not shown). Together, these findings suggested that between E15.5 and P2, after the peak of NOCD, a group of recombined-*met* neurons had been eliminated, and that Met signaling might be required for the survival of a specific MN population confined to the C8–T1 region.

However, it remained necessary to confirm that the Met-positive cells missing in *Nes-Met*$^{LacZ/fl}$ spinal cords at P2 were indeed MNs, and to exclude the possibility that the reduction in *lacZ*-positive cell numbers was due to altered expression of the reporter gene. We therefore quantified MN numbers at different stages using *in situ* hybridization with a *ChAT* riboprobe. Similar MN numbers were observed in mutants and controls at E15.5 (data not shown), as expected. However, by P2, there was a significant reduction in *Nes-Met*$^{fl/d}$ (22.4 ± 1.8% loss) and in *Nes-Met*$^{fl/LacZ}$ mutants (data not shown) as compared to controls (Fig. 7*A*–*C*). As with *LacZ*-labeled neurons, the loss was limited to C8–T1 levels (Fig. 7*C*). In adult mice, no further reduction in MN number was observed (17.1 ± 1.4% loss; data not shown). Thus, inactivation of *met* after the peak of NOCD triggers the loss of a subgroup of MNs in the C8–T1 spinal cord segment.

MNs lost in the conditional *Nes-Met* mutants correspond to the most caudal subset in the brachial spinal cord

We next asked whether MNs lost in the conditional *met* mutants corresponded to a specific motor pool and whether they might exhibit a shared molecular identity. Given the known coexpression of *met* with *pea3* in the caudal part of the *pea3* expression domain, we confirmed at E15.5 and P2 that recombined-*met* neurons identified by β-galactosidase activity colocalize with *pea3* (identified by *in situ* hybridization; data not shown). We therefore sought to determine whether the C8–T1 neurons missing at P2 in *Nes-Met*$^{fl/d}$ mutants corresponded to subsets of *pea3*-positive MNs. Although the level of *pea3* expression is maximal at developmental stages E11 to E16 and progressively diminishes, it is still possible to detect *pea3* mRNA levels in MNs (as well as in small cells of glial appearance throughout the spinal cord) at P2. Quantification revealed a significant reduction in the number of *pea3*-positive MNs in the *Nes-Met*$^{fl/d}$ spinal cords, once again in the region comprising the end of C8 to T1 segments (Fig. 8*A*–*D*,*I*). This corresponds to the most posterior region of the *pea3* domain, which did not match with the known anteroposterior extent of either the cutaneous maximus (C7–T1) or latissimus dorsi (C7) motor pools (Vrieseling and Arber, 2006).

Since the loss of MNs was quantitatively and spatially restricted, we asked whether they might correspond to a specific subset of those that normally express Met. To distinguish them among the *pea3*-expressing MNs and determine their identity with respect to the pool expressing *runx1*, we took advantage of a *nls-LacZ* insertion in the *runx1* locus (Roth et al., 1999). Notably, quantification of *runx1*-positive MN numbers revealed no significant changes in the *Nes-Met*$^{fl/d}$;*runx1*$^{LacZ/+}$ mutants compared to *runx1*$^{LacZ/+}$ control mice (Fig. 8*E–H,J*). Thus, the MNs whose survival is dependent on Met are distinguishable by their *met*$^{+}$;*pea3*$^{+}$;*runx1*$^{-}$ molecular identity and appear to correspond to the more caudal of the two Met-expressing groups defined in our expression study. Our findings are consistent with the idea that the Met-dependent MNs constitute a pool, which maps to the C8–T1 level and projects to an as yet unidentified muscle. Given the small number of neurons that are lost in Met mutants, our prediction was that this was most likely a small muscle.

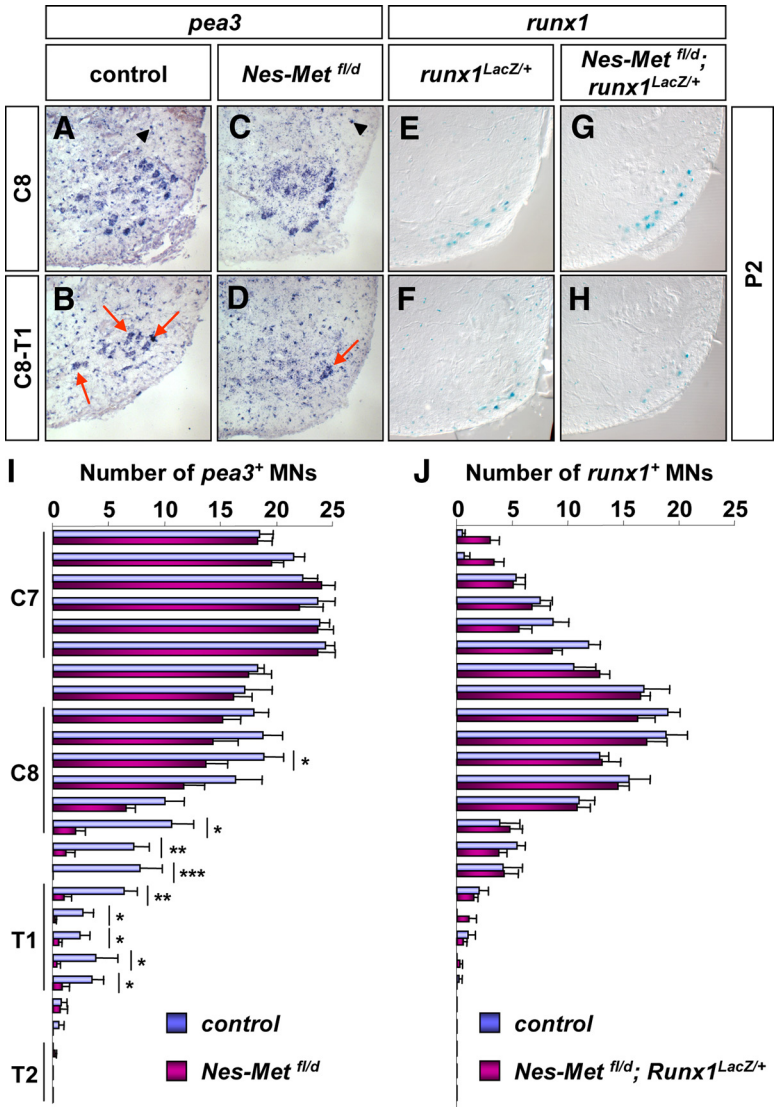

Figure 8. Loss of *pea3*-positive MNs in newborn *Nes-Met*$^{fl/d}$ mutants. ***A–D***, *In situ* hybridization performed using riboprobes for *pea3* on serial cross sections of newborn (P2) *Nes-Met*$^{fl/d}$ mutants ($n = 3$) and control (*Nes-Met*$^{fl/+}$) littermates ($n = 3$). At P2, *pea3* is expressed both in MNs (red arrow) and in glial cells (black arrowhead). ***E–H***, Representative images of β-galactosidase activity performed on cross sections of P2 spinal cords of *Nes-Met*$^{fl/d}$;*runx1*$^{LacZ/+}$ mutants ($n = 4$) and *runx1*$^{LacZ/+}$ controls ($n = 4$). ***I***, Quantification analysis showing a reduction in *pea3*-positive MN numbers specifically in the region spanning from the end of C8 to the T1 of the *Nes-Met*$^{fl/d}$ mutants. The position of the C7–T2 spinal segments is indicated. ***J***, Quantification showing no significant difference in the number of *runx1*-positive MNs in the two groups of animals analyzed. Student's *t* test: $^{*}p < 0.05$, $^{**}p < 0.01$, $^{***}p < 0.001$. Error bars represent SEM.

Reduced motor axon arborization in the pectoralis minor muscle of conditional *Nes-Met* mutants

As a step toward identifying the muscle innervated by the Met-dependent motor pool, we next asked whether the loss of C8–T1 MN group in *Nes-Met*$^{fl/d}$ mutants was accompanied by a defect in innervation of a specific muscle. We performed anti-neurofilament staining on muscles dissected from newborn *Nes-Met*$^{fl/d}$ and controls. Although the affected MN pool belongs to the *pea3* domain (Livet et al., 2002; Helmbacher et al., 2003), no significant alterations of the pattern of nerve terminals were found in the known *pea3* target muscles cutaneous maximus or latissimus dorsi (data not shown), as expected from the unchanged numbers of *runx1*-positive MNs, and from the anteroposterior position of MNs innervating these muscles. Moreover, the innervation pattern of the pectoralis major, a pectoral muscle known to receive axonal projections from *pea3*-negative C7–C8 MNs, but to be indirectly influenced by defects in *pea3* MNs (Vrieseling and Arber, 2006), was also unaffected (data not shown).

The target muscle of the Met-dependent C8–T1 MNs should be innervated by axons from *pea3*-expressing MNs. Staining for β-galactosidase activity in *pea3*^{tauLacZ} reporter mice previously ruled out the presence of LacZ^{+} axons in the limb (Livet et al., 2002). Because *pea3* motor pools nevertheless belong to the lateral motor column, we focused on pectoral belt muscles, which receive lateral motor column innervation. We considered the pectoralis minor muscle, a small muscle not included in previous studies in mouse, as one candidate, presuming that its C8–T1 innervation reported in human is conserved in mouse. Using anti-neurofilament staining on dissected pectoralis minor, we found a significant reduction in its axonal arborization profile in *Nes-Met*$^{fl/d}$ mutants compared to controls, as assessed by quantifying both the length and the number of branches of primary and second order (Fig. 9). The reduced profile of axonal arborization, which provides an indication on the number of axons/MNs, suggests a reduced motor pool size in *Nes-Met*$^{fl/d}$ mutants. As such an innervation defect was not seen in other muscles, the loss is likely to be confined to one motor pool rather than distributed among several pools.

To determine whether the pectoralis minor is indeed innervated by *pea3*-expressing MNs, we generated a transgenic mouse in which the GFP reporter gene has been inserted into the *pea3* locus in a large BAC encompassing the gene and the surrounding genome (Fig. 10*A* and data not shown) (since the official name of the *pea3* locus is *Etv4*, we refer to the BAC-transgene as *Etv4*-

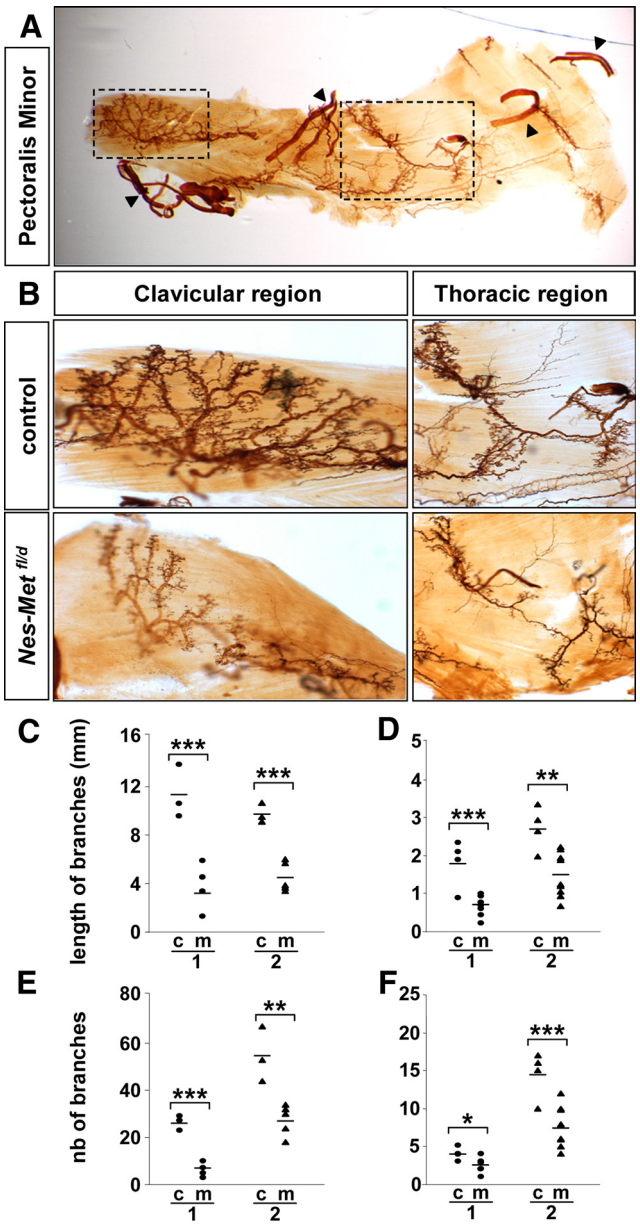

Figure 9. Innervation defects of the pectoralis minor muscle in the *Nes-Met*$^{fl/d}$ mutant mice. ***A***, ***B***, Whole-mount anti-neurofilament labeling of the pectoralis minor muscle in newborn controls and *Nes-Met*$^{fl/d}$ mutants. The innervation of the pectoralis minor muscle can be subdivided in two main areas, the clavicular and the thoracic region (depicted by the dashed lines). High magnification of these regions is shown. In control animals, the innervation pattern shows complex ramifications, whereas in *Nes-Met*$^{fl/d}$ mutants motor branches are severely reduced in number and length. The black arrowheads in ***A*** indicate sensory nerve branches. ***C–F***, Axonal arborization was quantified using the NeuronJ plugin of ImageJ. The graphs show the length (***C***, ***D***) and number (***E***, ***F***) of branches of primary (1) and secondary (2) order in the clavicular (***C***, ***E***) and thoracic (***D***, ***F***) region of control (c) and mutant (m) animals. Student's *t* test: $*p < 0.05$, $**p < 0.01$, $***p < 0.001$.

EGFP to avoid confusion with the endogenous *pea3* locus). The EGFP reporter in *Etv4-EGFP* mice fully recapitulates the *pea3* expression domain in the spinal cord and in other known domains (Fig. 10 and data not shown). In the BAC transgene, the EGFP fusion was designed such that the EGFP-tag replaces the *pea3* ETS domain, known to mediate DNA binding, and to be required for nuclear localization of Pea3 (Fig. 10*A*) (Janknecht, 1996; Janknecht et al., 1996). Therefore, the Pea3-EGFP fusion protein produced by the BAC is not retained in the nucleus, allowing EGFP staining of the cytoplasm and axons (Fig. 10*C–I* and data not shown). Thus, the *Etv4-EGFP* transgenic provides an excellent tool to precisely map the target muscles of *pea3* motor pools, refining the results obtained by retrograde tracing (Vrieseling and Arber, 2006). As expected, we observed EGFP-positive axons in the cutaneous maximus, both at E12 and at E17.5 (Fig. 10*E–I* and data not shown), as well as in the latissimus dorsi and some in the pectoralis major (data not shown). Overall examination of the EGFP signal in the pectoralis minor at E17.5 mostly revealed staining in tendons and muscle spindles, two previously reported sites of *pea3* expression in muscles (Fig. 11) (Hippenmeyer et al., 2002; Brent and Tabin, 2004). At higher magnification, however, EGFP-positive axons colocalized with anti-neurofilament staining (Fig. 11). This result confirms that the pectoralis minor indeed receives axonal projections from *pea3*-expressing MNs.

We next determined the state of innervation of endplates of the pectoralis minor muscle at P2 and found an increased incidence of partially or completely denervated synapses in *Nes-Met*$^{fl/d}$ mutants as compared to controls (Fig. 12*A–D*). By contrast, no neuromuscular junction defects were observed in the pectoralis major of the *Nes-Met*$^{fl/d}$ mutants (Fig. 12*E*). Similar defects of endplate innervation were also found in adult mutants compared to control animals (Fig. 12*F–I* and data not shown). No evident sign of fiber atrophy was observed in the pectoralis minor muscle of *Nes-Met*$^{fl/d}$ mutants (data not shown). Consistently, the total number of NMJs in the pectoralis minor was not significantly reduced in *Nes-Met*$^{fl/d}$ mutants as compared to controls ($p > 0.05$). The fact that all myofibers are innervated despite the lost MNs suggests a compensatory mechanism ensured by the remaining MNs in the pectoralis minor pool.

Finally, we asked whether the altered axonal profile found in P2/adult *Nes-Met*$^{fl/d}$ mutants is a consequence of deficient innervation of the pectoralis minor muscle (reflecting Met requirement at early stages) or truly resulted from degeneration of axons following neuronal loss. We therefore examined the innervation pattern of the pectoralis minor muscle at early developmental stages by performing whole-mount anti-neurofilament staining. Although a branching pattern within the pectoralis minor cannot unambiguously be identified in wild-type embryos at E12.5, dissection of the brachial plexus and removal of limb and limb-innervating nerve branches allows the lateral and medial pectoral nerve branches (lpn and mpn, respectively) (Fig. 4*D*) to be recognized. The lpn and mpn emerge from the anterior and posterior parts of the plexus, respectively. Notably, we found that in contrast to cutaneous maximus axons, which are severely affected at E12.5, the mpn, which contains C8–T1 axons projecting toward both the pectoralis minor and pectoralis major muscles, was unaffected at the same stage in both the conditional *Nes-Met*$^{fl/d}$ and the *met*$^{d/d}$ loss-of-function mutants (Fig. 4*D*), even though both muscles were reported to be missing in the latter mutants (Prunotto et al., 2004). Furthermore, analysis of the pectoralis minor muscle at E15.5 revealed similar innervation pattern between *Nes-Met*$^{fl/d}$ and control embryos (Fig. 13), in contrast to the innervation defects found after birth (Fig. 9*A*).

Together, our findings indicate that Met is dispensable for initial axonal growth of MNs innervating the pectoralis minor muscle, in contrast to its known role in enhancing axonal growth of MNs innervating the latissimus dorsi and the cutaneous maximus (Ebens et al., 1996; Maina et al., 1997, 2001). Instead, MNs in the pectoralis minor pool are dependent on HGF/Met for their survival during late embryogenesis, and after the peak of NOCD, in contrast to latissimus dorsi and cutaneous maximus MN pools

that do not significantly require HGF/Met signaling for their survival (Fig. 14). The reduction in number of the pectoralis minor pool in conditional *Met* mutants leads to denervation of the target muscle that appears sufficient to explain the specific weakness observed in the wire hanging test (Fig. 3).

Discussion

Precise control of MN numbers on a pool-by-pool basis during development is likely a key step in building a functional motor system. Our data reveal that one neurotrophic factor is required for embryonic survival of a single motor pool in the brachial spinal cord. In the absence of neurotrophic support, these neurons—but not neighboring pools expressing the same receptor—undergo cell death, leading to functional deficits that are behaviorally significant. This demonstrates the exquisite degree to which outcomes of signaling by receptor tyrosine kinases are regulated on a cell-by-cell basis. Moreover, our results provide a model for one way in which the multiplicity of neurotrophic factors may allow for regulation of MN numbers in a pool-specific manner.

Subtype specificity in the survival requirement of MNs: the HGF/Met example

The cre-loxP-mediated conditional deletion of *met* in the nervous system used in this study (*Nes-Met$^{fl/d}$* mutants) allowed us bypassing the early developmental requirements for Met and to reveal that, within a developmental window encompassing E15 to P2, a selective population of MNs strictly depends on Met for survival. We showed that Met is dispensable for the survival of MNs projecting to the cutaneous maximus and the latissimus dorsi. In contrast, MNs of the pectoralis minor pool require functional Met receptor for their survival after the peak of NOCD (Fig. 14). As effective Met deletion in our genetic system occurs after E15.5, it remains to be established whether survival of the pectoralis minor pool depends on HGF, or on other trophic factor(s), during the peak of NOCD. These findings shed light on how a neurotrophic factor such as HGF acts on a subset of MNs and delineate the timeframe in which its trophic effects are exerted. However, they also raise intriguing questions about the mechanisms through which specificity is generated, and the requirements of MNs for trophic support at different stages of their maturation.

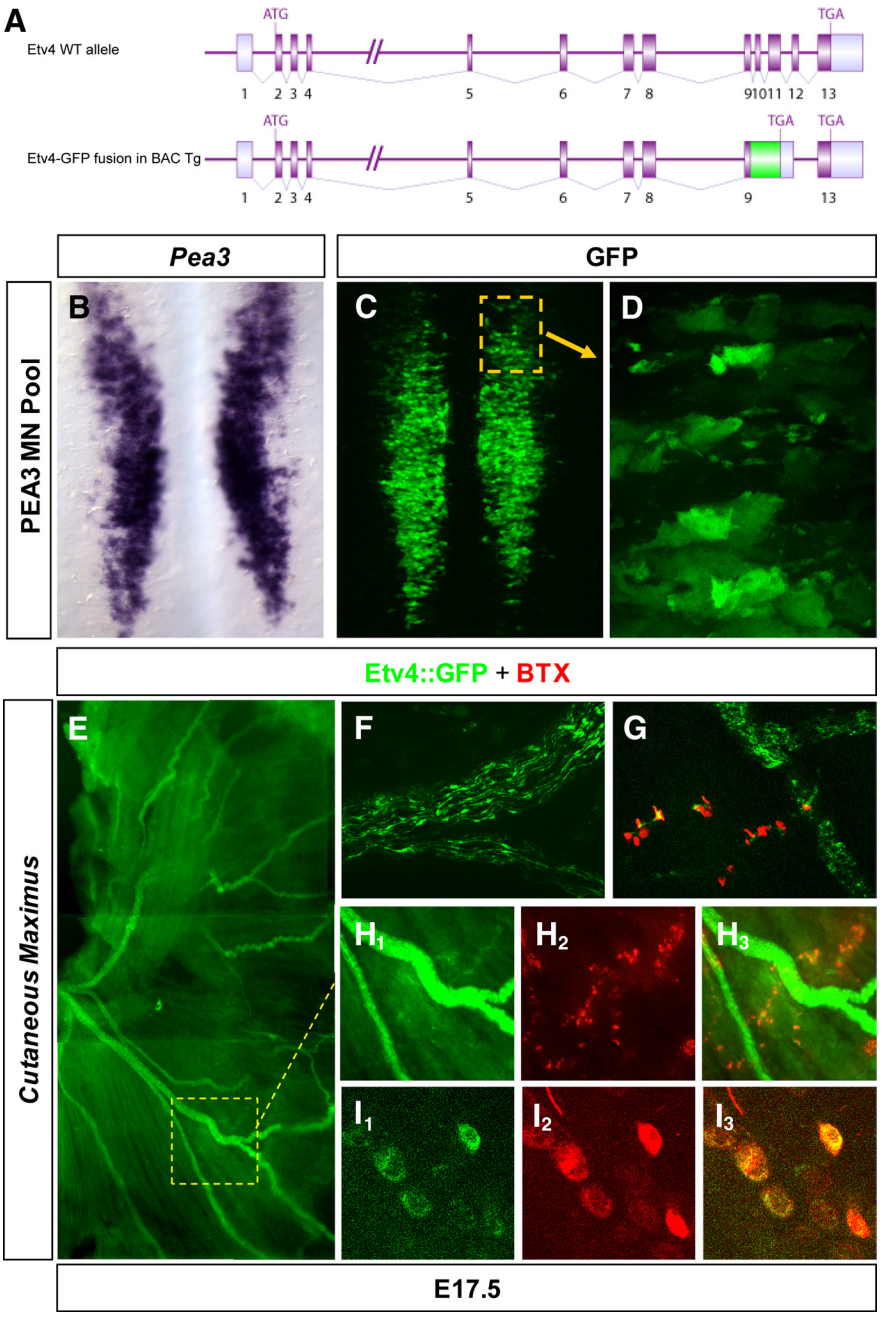

Figure 10. Generation of *Etv4:EGFP* mice and whole-mount imaging of EGFP-labeled axons and axon terminals in the cutaneous maximus. ***A***, Schematic representation of the strategy used. The *Etv4* locus is located on mouse chromosome 11. After fusion to the *EGFP* cassette (green), the resulting *Etv4-EGFP* fragment has been introduced into the BAC RP24–79P16. Genomic organization of the *Etv4* locus and localization of the site of insertion of the *EGFP* cassette (green), which has been inserted in frame with exon 9 of *Etv4*. The strategy also included the deletion of exons 10–13 of *Etv4* in the BAC, such that the *Etv4* locus is knocked out and does not lead to expression of functional Etv4 (Pea3) protein. ***B–D***, Histological analyses showing that EGFP expression reproduces the domain of *pea3* expression. Analysis of whole-mount spinal cord of E12.5 *Etv4-EGFP* embryos. Comparison between *in situ* hybridization using a *pea3* riboprobe (***B***) and direct observation of the GFP (***C***, ***D***) reveals that the strong EGFP expression faithfully recapitulates that of *pea3* transcripts. ***E***, Low-magnification view of ramifications of bundles of fluorescent axons in the CM. ***F***, High-magnification imaging shows that each bundle is composed of many individual axons. ***G–I***, α-Bungarotoxin staining of the NMJs (BTX, red) in combination with Etv4-EGFP labeling (green) of motor axon terminals reveal clusters of synapses innervated "en passant" by single axons (***G***, ***H_1–H_3***). ***I_1–I_3***, The PEA3-GFP fusion protein reaches and fills axon terminals, fully overlapping with the BTX-labeled (red) Acetylcholine receptor clusters.

The specificity of HGF dependency for MN survival within the *pea3* domain might potentially arise in the MNs themselves or from the target muscles. Previous studies followed the expression pattern of trophic factors in the target muscle and that of their

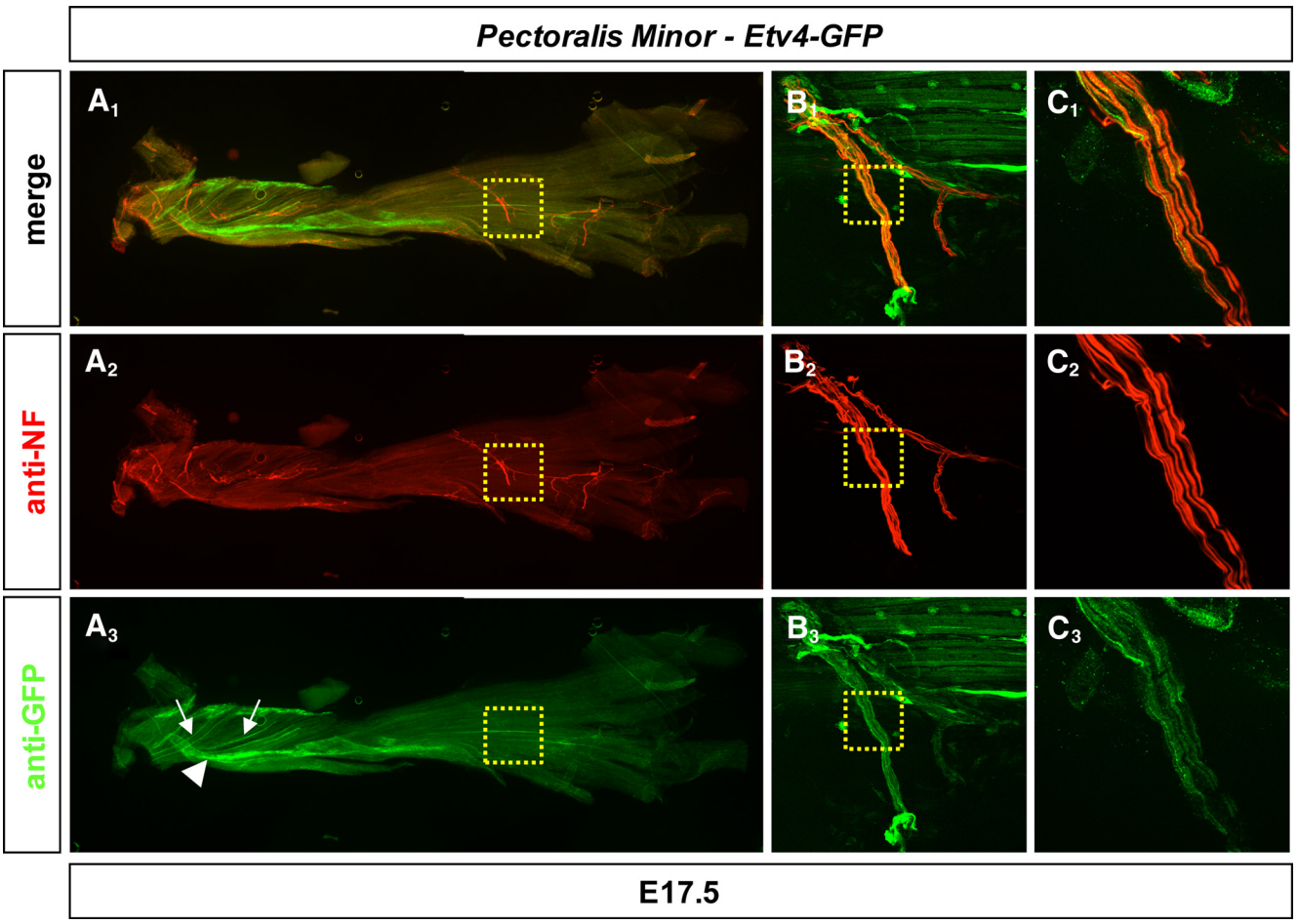

Figure 11. *pea3*-positive MNs innervate the pectoralis minor muscle. Fluorescence imaging of the pectoralis minor muscle of E17.5 *Etv4-EGFP* transgenic mice. Double immunostaining of the pectoralis minor was performed using anti-NF (red) and anti-EGFP (green) antibodies, and is shown with merged colours (1), or separate channels (2, anti-NF-red; 3 anti-GFP, green). ***A***, Observation of the entire muscle at low magnification shows that an EGFP signal is mostly seen in tendons (white arrowhead) and muscle spindles (white arrow). ***B***, ***C***, High magnification of the boxed areas in ***A*** and ***B***, respectively, showing colocalization of EGFP and NF in axons (green) of Pea3-MNs.

corresponding receptors in MNs (Gould and Oppenheim, 2004; Gu and Kania, 2010). The major conclusions from these studies were that (1) neurotrophic factors are present in muscles innervated by MNs that do not depend on these factors for survival; and (2) neurotrophic receptors are expressed in motor pools that do not depend on their corresponding ligands for their survival. One striking example is provided by Ret and GDNF, which are broadly expressed in MNs and muscles, respectively. Despite this, *gdnf*-deficient mice show a loss of only ~25% MNs (Moore et al., 1996; Oppenheim et al., 2000). Our data provide another illustration of this phenomenon: HGF is expressed in nearly all muscles [data not shown and Gu and Kania (2010)], and Met is expressed in several subsets of MNs, and yet only one brachial pool depends on Met for survival. Thus, expression of a given trophic ligand/receptor couple is necessary but not sufficient to determine populations in which the factor regulates survival.

An alternative explanation for the specificity of our observations could be that survival of other pools is ensured by a mixture of factors with redundant functions. For example, although Met is expressed by the cutaneous maximus and the latissimus dorsi pools and regulates key developmental processes in these neurons, it becomes dispensable for their survival later on. This finding suggests that other factors are required to sustain survival of this population. One possibility is that these pools are dependent on another trophic factor such as GDNF, which plays multiple roles in their development (Henderson et al., 1994; Springer et al., 1995; Haase et al., 2002; Gould et al., 2008; Shneider et al., 2009). However, current evidence suggests that GDNF exerts its survival activity principally on gamma MNs, making this hypothesis less probable. Moreover, lack of *pea3* induction in *gdnf* mutants precludes investigating directly whether GDNF supports the survival of the Pea3-positive MN pool. Another possibility is that HGF and GDNF exert redundant neurotrophic roles for the cutaneous maximus and the latissimus dorsi MN pools, thus reciprocally compensating for the loss of one another in single mutants.

Pleiotropic activities of HGF/Met: switching biological outcomes as a function of cell subtypes and time

Another alternative explanation for the pool specificity of HGF survival effects could be that Met signaling is modulated by the genetic context of the cell in which it is expressed and that only in pectoralis minor MNs it activates a survival pathway. In agreement with this, we previously illustrated the concept of pleiotropic use of an RTK system by showing that HGF/Met acts on selective signaling pathways to trigger qualitatively distinct biological outcomes in different tissues (Maina et al., 2001). Perhaps because of the need to strictly control its intrinsically pleiotropic properties, the HGF/Met biological response is imposed by the cell types in which it acts. For example, during embryogenesis, Met regulates survival in liver cells, whereas it is required for

proliferation and migration in muscle cells (Maina et al., 1996). We now provide another level of specificity for pleiotropic RTK functions. We show that, among Met-expressing MNs, Met is not required for the survival of subsets (cutaneous maximus and latissimus dorsi MNs), in which it triggers axon growth/guidance and transcriptional responses (*runx1* expression). However, it is necessary as a survival factor for the pectoralis minor MNs, in which it is dispensable for branching of this pectoral nerve (Fig. 14). This selective HGF/Met requirement within the same cell type (*pea3*-positive MNs) provides the most striking *in vivo* evidence so far that distinct subgroups of cells can make differential use of a pleiotropic factor for specific biological responses, such as identity acquisition, axonal growth, and survival.

Another aspect of our data implies a temporal control of neurotrophic signaling that may be important for a full understanding of the role of cell death and survival factors in shaping adult neuronal populations. The effects of HGF/Met on cell survival we report here occur after the well studied wave of NOCD at this level of the spinal cord (Yamamoto and Henderson, 1999). This suggests that HGF is required for the continued maintenance of those MNs in the pectoralis minor pool that have survived the initial wave of NOCD. This switch in function according to the developmental stage that we report here is reminiscent of our studies on dorsal root ganglion sensory neurons. Whereas at E12.5, Met regulates survival of a subpopulation of sensory neurons expressing the TrkA receptor (Maina et al., 1997), this trophic dependency is lost at later stages (Gascon et al., 2010). Instead, after birth, HGF/Met acts synergistically with nerve growth factor (NGF)/TrkA to promote expression of the peptidergic characteristics of a subset of nociceptive neurons (Gascon et al., 2010), through cross-repressive regulatory interactions with Runx1, in contrast to the positive regulation we report in MNs. Other neurotrophic factors may also contribute to maintenance of MN numbers after the period of naturally occurring cell death (Baudet et al., 2008; Lee et al., 2008). However, the degree to which these effects are pool specific was not determined.

Overall, our results provide novel insights into the role of neurotrophic factors in ensuring that subsets of MNs with specific adult functions are maintained throughout life. They suggest that the considerable degree of molecular diversity observed between MNs in different pools may not only serve for correct projections and circuit formation during early embryogenesis, but could potentially be required for appropriate pool-specific modulation of the outcome of signaling by Met and other RTK receptors. It was already known that some factors such as GDNF play pool-specific roles in MN positioning, axon growth, and circuit formation. Our data raise the possibility that different neurotrophic factors are also required for the survival of different groups of MNs. This provides a way in which the elegantly simple neurotrophic hypothesis first put forward for MNs by Levi-Montalcini (1987) may be modified to encompass our growing understanding of the functional and molecular diversity of spinal MNs.

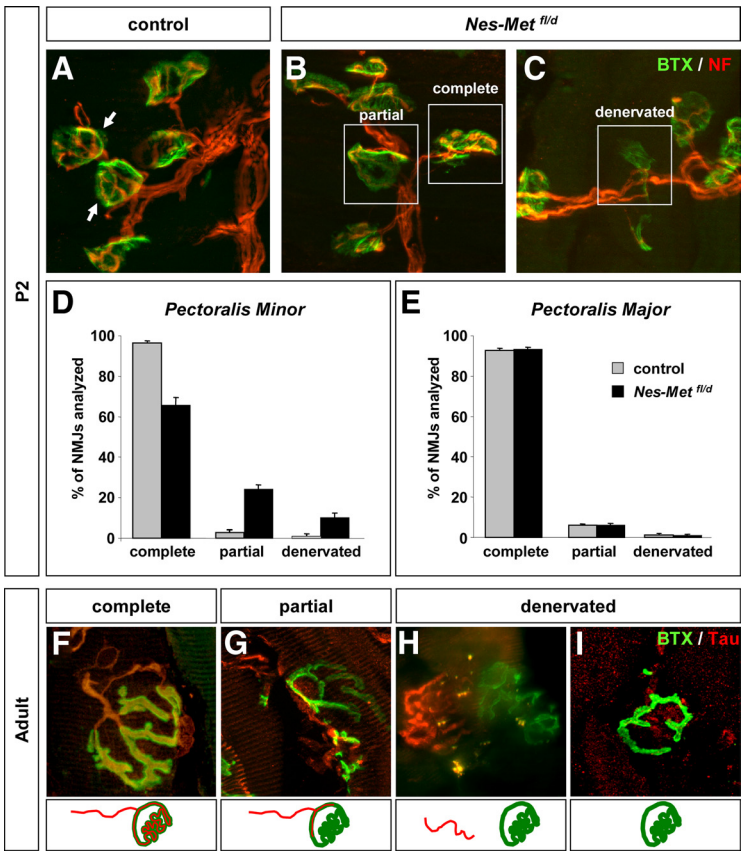

Figure 12. Pectoralis minor innervation defects in P2 and adult *Nes-Met*$^{fl/d}$ mutants. NMJs were analyzed both in the pectoralis minor and in the pectoralis major muscles of P2 (***A–E***) and adult (***F–I***) *Nes-Met*$^{fl/d}$ mutants and control (*Nes-Met*$^{fl/+}$) littermates ($n = 6$ for each P2 group, and $n = 3$ for each adult group). ***A–C***, NMJs form very large and complex pretzel-shape structures that overlap with the endplate of the axon. Motor endplates and axons were visualized with α-BTX (green) and anti-NF antibodies (red), respectively. Confocal images depict fully innervated, partially innervated, and denervated endplates (squares in ***B*** and ***C***). ***D***, ***E***, Quantitative analysis of NMJ innervation of *Nes-Met*$^{fl/d}$ mutant and control (*Nes-Met*$^{fl/+}$) mice in the pectoralis minor (***D***) and in the pectoralis major (***E***) muscles. Data are shown as percentage of NMJs classified as completely, partially innervated, or totally denervated. ***F–I***, Partially innervated and denervated endplates were also found in adult *Nes-Met*$^{fl/d}$ mutants. Below each image is a schematic representation of the innervation status.

References

Arce V, Garces A, de Bovis B, Filippi P, Henderson C, Pettmann B, deLapeyrière O (1999) Cardiotrophin-1 requires LIFRbeta to promote survival of mouse motoneurons purified by a novel technique. J Neurosci Res 55:119–126.

Baudet C, Pozas E, Adameyko I, Andersson E, Ericson J, Ernfors P (2008) Retrograde signaling onto Ret during motor nerve terminal maturation. J Neurosci 28:963–975.

Bladt F, Riethmacher D, Isenmann S, Aguzzi A, Birchmeier C (1995) Essential role for the c-*met* receptor in the migration of myogenic precursor cells into the limb bud. Nature 376:768–771.

Brent AE, Tabin CJ (2004) FGF acts directly on the somitic tendon progenitors through the Ets transcription factors Pea3 and Erm to regulate sclerotome axis expression. Development 131:3885–3896.

Caton A, Hacker A, Naeem A, Livet J, Maina F, Bladt F, Klein R, Birchmeier C, Guthrie S (2000) The branchial arches and HGF are growth-promoting and chemoattractant for cranial motor axons. Development 127:1751–1766.

Dasen JS, Jessell TM (2009) Hox networks and the origins of motor neuron diversity. Curr Top Dev Biol 88:169–200.

Dasen JS, Tice BC, Brenner-Morton S, Jessell TM (2005) A Hox regulatory

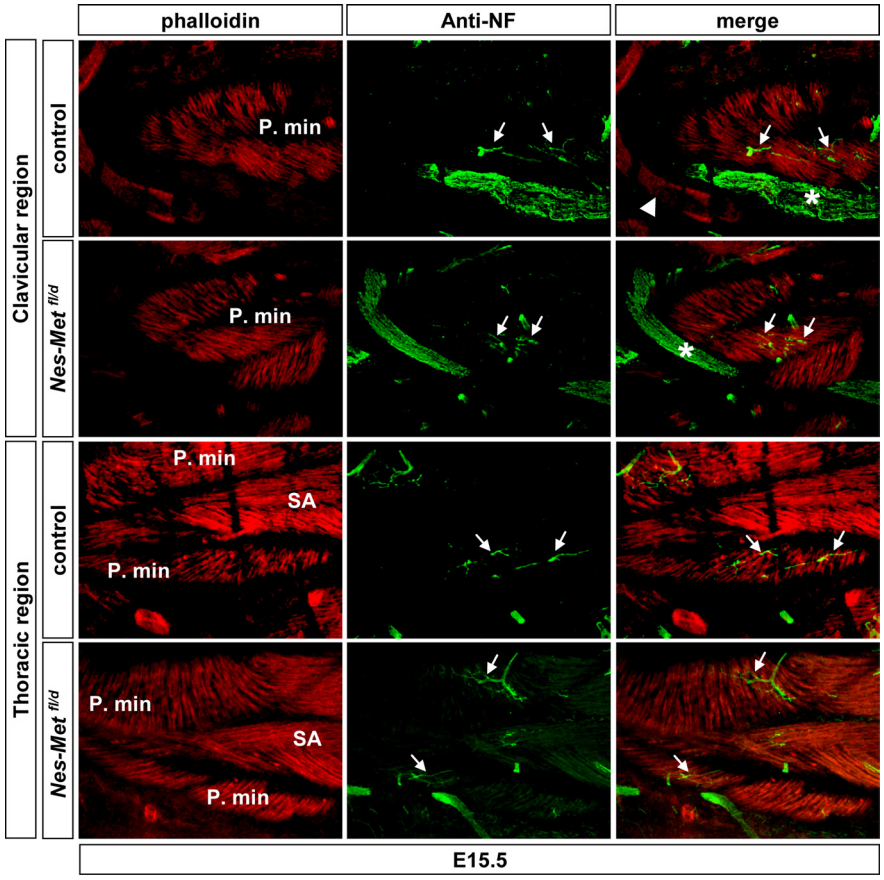

Figure 13. Innervation of the pectoralis minor muscle is preserved at E15.5 in *Nes-Met*$^{fl/d}$ mutants. Cross section of E15.5 embryos were subjected to double immunostaining using phalloidin and anti-NF antibodies. The innervation pattern of the pectoralis minor muscle (P.min; white arrow) was similar in *Nes-Met*$^{fl/d}$ mutants and control (*Nes-Met*$^{fl/+}$) littermates both in the clavicular and thoracic regions ($n = 3$ for each group). Position of the serratus anterior (SA) muscle is indicated. The asterisk shows the brachial plexus. The clavicle is indicated by the white arrowhead.

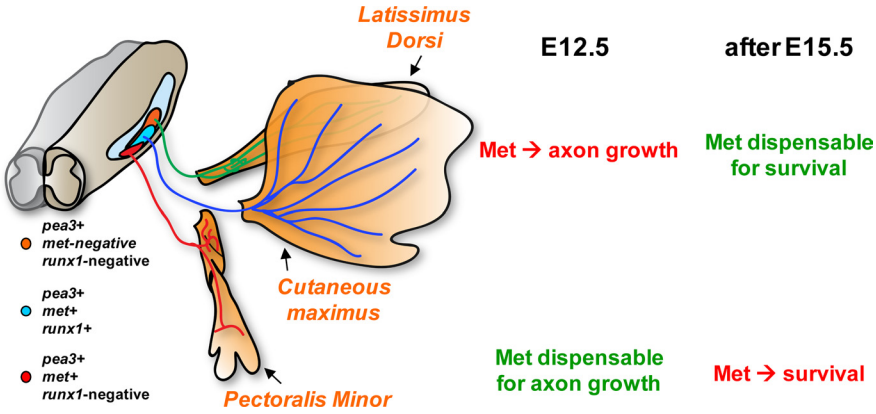

Figure 14. Pleiotropic activities of HGF/Met in pea3-positive motor neurons: switching biological outcomes as a function of cell subtypes and time. The MN pool expressing *pea3*, *met*, and *runx1* (*pea3*$^+$, *met*$^+$, *runx1*$^+$; dark blue pool) innervates the cutaneous maximus, and depends on the HGF/Met system at early developmental stages (E12) for axonal growth/guidance and gene expression (*runx1*). The MN pool expressing *pea3* only (*pea3*$^+$, *met*-negative, *runx1*-negative; orange pool) innervates the latissimus dorsi, and depends on the HGF/Met system at early developmental stages (E12) for axonal growth/guidance. At later developmental stages, HGF/Met becomes dispensable for the survival of both cutaneous maximus and latissimus dorsi pools. The pool consisting of MNs expressing *pea3* and *met*, but not *runx1* (*pea3*$^+$, *met*$^+$, *runx1*-negative; red pool) is located at the most caudal level (C8–T1). These MNs innervate the pectoralis minor muscle in an HGF/Met-independent manner, and acquire dependency on HGF/Met for their survival at late stage of development (after E15.5).

network establishes motor neuron pool identity and target-muscle connectivity. Cell 123:477–491.
Ebens A, Brose K, Leonardo ED, Hanson MG Jr, Bladt F, Birchmeier C, Barres BA, Tessier-Lavigne M (1996) Hepatocyte growth factor/Scatter factor is an axonal chemoattractant and a neurotrophic factor for spinal motor neurons. Neuron 17:1157–1172.
Furlan A, Stagni V, Hussain A, Richelme S, Conti F, Prodosmo A, Destro A, Roncalli M, Barila D, Maina F (2011) Abl interconnects oncogenic Met and p53 core pathways in cancer cells. Cell Death Differ. Advance online publication. doi:10.1038/cdd.2011.23.
Gascon E, Gaillard S, Malapert P, Liu Y, Rodat-Despoix L, Samokhvalov IM, Delmas P, Helmbacher F, Maina F, Moqrich A (2010) Hepatocyte growth factor-Met signaling is required for Runx1 extinction and peptidergic differentiation in primary nociceptive neurons. J Neurosci 30:12414–12423.
Genestine M, Caricati E, Fico A, Richelme S, Hassani H, Sunyach C, Lamballe F, Panzica GC, Pettmann B, Helmbacher F, Raoul C, Maina F, Dono R (2011) Enhanced neuronal Met signalling levels in ALS mice delay disease onset. Cell Death Dis 2:e130.
Gong S, Yang XW, Li C, Heintz N (2002) Highly efficient modification of bacterial artificial chromosomes (BACs) using novel shuttle vectors containing the R6Kgamma origin of replication. Genome Res 12:1992–1998.
Gould TW, Oppenheim RW (2004) The function of neurotrophic factor receptors expressed by the developing adductor motor pool *in vivo*. J Neurosci 24:4668–4682.
Gould TW, Yonemura S, Oppenheim RW, Ohmori S, Enomoto H (2008) The neurotrophic effects of glial cell line-derived neurotrophic factor on spinal motoneurons are restricted to fusimotor subtypes. J Neurosci 28:2131–2146.
Gu WX, Kania A (2010) Examining the combinatorial model of motor neuron survival by expression profiling of trophic factors and their receptors in the embryonic *Gallus gallus*. Dev Dyn 239:965–979.
Haase G, Dessaud E, Garcès A, de Bovis B, Birling M, Filippi P, Schmalbruch H, Arber S, deLapeyrière O (2002) GDNF acts through PEA3 to regulate cell body positioning and muscle innervation of specific motor neuron pools. Neuron 35:893–905.
Helmbacher F, Dessaud E, Arber S, deLapeyrière O, Henderson CE, Klein R, Maina F (2003) Met signaling is required for recruitment of motor neurons to PEA3-positive motor pools. Neuron 39:767–777.
Henderson CE (1996) Programmed cell death in the developing nervous system. Neuron 17:579–585.
Henderson CE, Phillips HS, Pollock RA, Davies AM, Lemeulle C, Armanini M, Simpson LC, Moffet B, Vandlen RA, Koliatsov VE, Rosenthal A (1994) GDNF: a potent survival factor for motoneurons present in peripheral nerve and muscle. Science 266:1062–1064.
Hippenmeyer S, Shneider NA, Birchmeier C, Burden SJ, Jessell TM, Arber S (2002) A role for neuregulin1 signaling in muscle spindle differentiation. Neuron 36:1035–1049.
Huh CG, Factor VM, Sánchez A, Uchida K, Conner

EA, Thorgeirsson SS (2004) Hepatocyte growth factor/c-met signaling pathway is required for efficient liver regeneration and repair. Proc Natl Acad Sci U S A 101:4477–4482.

Janknecht R (1996) Analysis of the ERK-stimulated ETS transcription factor ER81. Mol Cell Biol 16:1550–1556.

Janknecht R, Monté D, Baert JL, de Launoit Y (1996) The ETS-related transcription factor ERM is a nuclear target of signaling cascades involving MAPK and PKA. Oncogene 13:1745–1754.

Jessell TM (2000) Neuronal specification in the spinal cord: inductive signals and transcriptional codes. Nat Rev Genet 1:20–29.

Kablar B, Rudnicki MA (1999) Development in the absence of skeletal muscle results in the sequential ablation of motor neurons from the spinal cord to the brain. Dev Biol 208:93–109.

Kanning KC, Kaplan A, Henderson CE (2010) Motor neuron diversity in development and disease. Annu Rev Neurosci 33:409–440.

Koyama J, Yokouchi K, Fukushima N, Kawagishi K, Higashiyama F, Moriizumi T (2003) Neurotrophic effect of hepatocyte growth factor on neonatal facial motor neurons. Neurol Res 25:701–707.

Kramer ER, Knott L, Su F, Dessaud E, Krull CE, Helmbacher F, Klein R (2006) Cooperation between GDNF/Ret and ephrinA/EphA4 signals for motor-axon pathway selection in the limb. Neuron 50:35–47.

Landmesser L (1978) The distribution of motoneurones supplying chick hind limb muscles. J Physiol 284:371–389.

Lee N, Robitz R, Zurbrugg RJ, Karpman AM, Mahler AM, Cronier SA, Vesey R, Spearry RP, Zolotukhin S, Maclennan AJ (2008) Conditional, genetic disruption of ciliary neurotrophic factor receptors reveals a role in adult motor neuron survival. Eur J Neurosci 27:2830–2837.

Levi-Montalcini R (1987) The nerve growth factor 35 years later. Science 237:1154–1162.

Livet J, Sigrist M, Stroebel S, De Paola V, Price SR, Henderson CE, Jessell TM, Arber S (2002) ETS gene Pea3 controls the central position and terminal arborization of specific motor neuron pools. Neuron 35:877–892.

Maina F, Klein R (1999) Hepatocyte growth factor—a versatile signal for developing neurons. Nat Neurosci 2:213–217.

Maina F, Casagranda F, Audero E, Simeone A, Comoglio PM, Klein R, Ponzetto C (1996) Uncoupling of Grb2 from the Met receptor in vivo reveals complex roles in muscle development. Cell 87:531–542.

Maina F, Hilton MC, Ponzetto C, Davies AM, Klein R (1997) Met receptor signaling is required for sensory nerve development and HGF promotes axonal growth and survival of sensory neurons. Genes Dev 11:3341–3350.

Maina F, Hilton MC, Andres R, Wyatt S, Klein R, Davies AM (1998) Multiple roles for hepatocyte growth factor in sympathetic neuron development. Neuron 20:835–846.

Maina F, Panté G, Helmbacher F, Andres R, Porthin A, Davies AM, Ponzetto C, Klein R (2001) Coupling Met to specific pathways results in distinct developmental outcomes. Mol Cell 7:1293–1306.

Meijering E, Jacob M, Sarria JC, Steiner P, Hirling H, Unser M (2004) Design and validation of a tool for neurite tracing and analysis in fluorescence microscopy images. Cytometry A 58:167–176.

Moore MW, Klein RD, Fariñas I, Sauer H, Armanini M, Phillips H, Reichardt LF, Ryan AM, Carver-Moore K, Rosenthal A (1996) Renal and neuronal abnormalities in mice lacking GDNF. Nature 382:76–79.

Moumen A, Patané S, Porras A, Dono R, Maina F (2007a) Met acts on Mdm2 via mTOR to signal cell survival during development. Development 134:1443–1451.

Moumen A, Ieraci A, Patané S, Solé C, Comella JX, Dono R, Maina F (2007b) Met signals hepatocyte survival by preventing Fas-triggered FLIP degradation in a PI3k-Akt-dependent manner. Hepatology 45:1210–1217.

North T, Gu TL, Stacy T, Wang Q, Howard L, Binder M, Marín-Padilla M, Speck NA (1999) Cbfa2 is required for the formation of intra-aortic hematopoietic clusters. Development 126:2563–2575.

Novak KD, Prevette D, Wang S, Gould TW, Oppenheim RW (2000) Hepatocyte growth factor/scatter factor is a neurotrophic survival factor for lumbar but not for other somatic motoneurons in the chick embryo. J Neurosci 20:326–337.

Oppenheim RW (1996) Neurotrophic survival molecules for motoneurons: an embarrassment of riches. Neuron 17:195–197.

Oppenheim RW, Houenou LJ, Parsadanian AS, Prevette D, Snider WD, Shen L (2000) Glial cell line-derived neurotrophic factor and developing mammalian motoneurons: regulation of programmed cell death among motoneuron subtypes. J Neurosci 20:5001–5011.

Prunotto C, Crepaldi T, Forni PE, Ieraci A, Kelly RG, Tajbakhsh S, Buckingham M, Ponzetto C (2004) Analysis of Mlc-lacZ Met mutants highlights the essential function of Met for migratory precursors of hypaxial muscles and reveals a role for Met in the development of hyoid arch-derived facial muscles. Dev Dyn 231:582–591.

Roth W, Isenmann S, Naumann U, Kügler S, Bähr M, Dichgans J, Ashkenazi A, Weller M (1999) Locoregional Apo2L/TRAIL eradicates intracranial human malignant glioma xenografts in athymic mice in the absence of neurotoxicity. Biochem Biophys Res Commun 265:479–483.

Segarra J, Balenci L, Drenth T, Maina F, Lamballe F (2006) Combined signaling through ERK, PI3K/AKT, and RAC1/p38 is required for Met-triggered cortical neuron migration. J Biol Chem 281:4771–4778.

Shneider NA, Brown MN, Smith CA, Pickel J, Alvarez FJ (2009) Gamma motor neurons express distinct genetic markers at birth and require muscle spindle-derived GDNF for postnatal survival. Neural Dev 4:42.

Springer JE, Seeburger JL, He J, Gabrea A, Blankenhorn EP, Bergman LW (1995) cDNA sequence and differential mRNA regulation of two forms of glial cell line-derived neurotrophic factor in Schwann cells and rat skeletal muscle. Exp Neurol 131:47–52.

Stifani N, Freitas AR, Liakhovitskaia A, Medvinsky A, Kania A, Stifani S (2008) Suppression of interneuron programs and maintenance of selected spinal motor neuron fates by the transcription factor AML1/Runx1. Proc Natl Acad Sci U S A 105:6451–6456.

Tronche F, Kellendonk C, Kretz O, Gass P, Anlag K, Orban PC, Bock R, Klein R, Schütz G (1999) Disruption of the glucocorticoid receptor gene in the nervous system results in reduced anxiety. Nat Genet 23:99–103.

Vrieseling E, Arber S (2006) Target-induced transcriptional control of dendritic patterning and connectivity in motor neurons by the ETS gene Pea3. Cell 127:1439–1452.

Wong V, Glass DJ, Arriaga R, Yancopoulos GD, Lindsay RM, Conn G (1997) Hepatocyte growth factor promotes motor neuron survival and synergizes with ciliary neurotrophic factor. J Biol Chem 272:5187–5191.

Yamamoto Y, Henderson CE (1999) Patterns of programmed cell death in populations of developing spinal motoneurons in chicken, mouse, and rat. Dev Biol 214:60–71.

Yamamoto Y, Livet J, Pollock RA, Garces A, Arce V, deLapeyrière O, Henderson CE (1997) Hepatocyte growth factor (HGF/SF) is a muscle-derived survival factor for a subpopulation of embryonic motoneurons. Development 124:2903–2913.